GEOLOGICAL SURVEY OF CANADA
OPEN FILE 7456

Crustal Structure in the Gulf of St. Lawrence Region, Eastern Canada: Preliminary Results From Receiver Function Analysis

H. Kao, S.-J. Shan, J.F. Cassidy, and S.A. Dehler

2014

GEOLOGICAL SURVEY OF CANADA
OPEN FILE 7456

Crustal Structure in the Gulf of St. Lawrence Region, Eastern Canada: Preliminary Results From Receiver Function Analysis

H. Kao, S.-J. Shan, J.F. Cassidy, and S.A. Dehler

2014

doi:10.4095/293724

Recommended citation
Kao, H., Shan, S.-J., Cassidy, J.F., and Dehler, S.A., 2014. Crustal structure in the Gulf of St. Lawrence region, Eastern Canada: Preliminary results from receiver function analysis; Geological Survey of Canada, Open File 7456, 48 p. doi:10.4095/293724

Crustal Structure in the Gulf of St. Lawrence Region, Eastern Canada: Preliminary Results From Receiver Function Analysis

H. Kao[1], S.-J. Shan[1], J.F. Cassidy[1], and S.A. Dehler[2]

[1]Geological Survey of Canada, Pacific Division, Sidney, BC, V8L 4B2

[2]Geological Survey of Canada, Atlantic Division, Dartmouth, NS, B2Y 4A2

1. Introduction

The Gulf of St. Lawrence (GSL) is located in easternmost Canada, surrounded by Quebec and the Atlantic provinces (Figure 1). This region has experienced a complex geologic evolution that involved two cycles of ocean closure and opening during the Phanerozoic (e.g., Williams et al., 1999). In addition, Grenvillian collision has had a major impact on the geological structure of the Prcambrian basement. Major geological events during the Phaneroizoic included the formation of the Appalachian mountains and the development of a modern continental margin (e.g., Hall et al., 1998). Previous studies of the deep crust in the region have been limited to a few marine wide-angle reflection and refraction profiles in the Gulf and multichannel seismic lines across Newfoundland collected as part of the LITHOPROBE program (e.g., Chian et al., 1998; Hughes et al., 1994; Marillier et al., 1991; Marillier et al., 1994; Quinlan et al., 1992). Many questions about the crustal structure of the region remain unresolved, including the nature and position of the contacts between the geological zones that comprise the Appalachians, the thinning of the crust and lithosphere associated with basin formation, the velocity structure and physical properties of the crustal rocks, and the variations in the thickness of upper crustal sedimentary successions. Our study can bring additional controls on Appalachian crustal structures that could result in better estimates of heat flow from the mantle through the crust and sedimentary rocks at the time the basins formed, and ultimately could help define models of basin evolution.

With the support from the Portable Observatories for Lithospheric Analysis and Research Investigating Seismicity (POLARIS) Consortium, the Geological Survey of Canada (GSC) deployed a temporary seismic array consisting of ten broadband stations in the GSL region between fall 2005 and 2008 (called therein “the temporary Atlantic array”; red triangles, Figure 1). There are also permanent seismograph stations in the region that belong to the Canadian National Seismograph Network (CNSN; blue triangles, Figure 1). Some stations have been in operation for decades in analogue mode, and conversion to three-component broadband digital recording started in the early 1990's. These broadband stations are ideal for seismic receiver function analysis using sources located at teleseismic distances between 30 and 100 degrees. In addition, data recorded at the new stations aid in the positioning and analysis of local and regional seismic events. In this report, we describe the results of the passive source seismic data collection, processing, and the preliminary conclusions of receiver function analysis.

2. Station Information

The temporary Atlantic array consisted of 10 seismograph stations that were installed in the fall of 2005. Table 1 lists each station's geographic location, longitude, latitude, elevation, and operation period. Each station used a digital, three-component broadband seismometer, an instrument that record ground motions. The stations also included a satellite communications system and a power source, typically a battery bank charged by solar panels (Figure 2). Data were transmitted in real-time via satellite to data centres in Ontario maintained by the POLARIS Consortium. All seismometers were emplaced on a concrete base. Depending on the individual geological conditions, bedrock sites were chosen if available.

A brief summary of the geological setting, based on geological mapping and reflection/refraction interpretations, of each station site is given below.

CODG (Codroy, NL): Located on the eastern edge of Carboniferous (Maritimes) basin, north of a major fault connecting through the northern tip of Cape Breton. V_p of the lower crust is 6.2 km/s (Jackson, 2002; Jackson et al., 1998). Moho depth is approximately 35 km (Jackson, 2002).

BATG (Bathurst, NB): Located on the western limit of the Carboniferous (Maritimes) basin, above the central block (Gardena) of the Appalachians. V_p of the lower crust is 6.2 km/s (Jackson, 2002; Jackson et al., 1998). Moho depth is approximately 35 km (Jackson, 2002).

CHEG (Cheticamp, NS): The bedrock site sits atop Cape Breton highlands. It is located to the south of a major fault.

GBN (Guysborough, NS): Adjacent to a major south-dipping fault, separating two terranes (Avalon and Meguma) with different crustal compositions and velocities.

MALG (Malagash, NS): Located on the southern edge of the Carboniferous (Maritimes) basin within the Avalon terrane.

TIGG (Tignish, PE): Underlain by Carboniferous (Maritimes) basin within the central block (Gardena). Upper crustal V_p is 6.2 km/s (Jackson, 2002). Moho depth is estimated to be approximately 35 km (Jackson, 2002).

MADG (Magdelan Islands, QC): Structural geology is primarily volcanic rubble, probably atop a salt diapir within a thick sedimentary sequence. In the central part of Carboniferous (Maritimes) basin. Upper crustal V_p is 6.2 km/s (Jackson, 2002). Moho depth is estimated to be approximately 35 km (Jackson, 2002).

GASG (Gaspe, QC): At the edge of Grenville Orogen. It is located in the Humber terrane with similar setting to DRLN. Thickness of the sedimentary layer is unknown. Extreme sedimentary deformation is exposed at road cut. V_p for upper crust is 6.2 km/s. Lower crust has a high V_p (7.2 km/s, Jackson et al., 1998). The thickness of the high velocity lower crustal layer is 10 km or more (Marillier et al., 1991).

NATG (Baie Johan Beetz, QC): Within the Grenville Orogen. Lower crust Vp is 6.7 km/s (Jackson et al., 1998). Moho depth is greater than 40 km (Jackson et al., 1998). Moho depth is estimated to be 42-44 km from gravity data (Marillier and Verhoef, 1989).

SABG (Sable Island, NS): Thickness of the sedimentary layer is unknown but could be in excess of 10 km. This site is located on sandy ground which may have given poor coupling to record ground motions. V_p of lower crust is between 6.7 and 6.9 km/s (Funck et al., 2004). The crustal thickness is estimated to be 25-30 km (Funck et al., 2004).

3. Data Collection and Processing

We searched the global earthquake database of the National Earthquake Information Center (NEIC) of the U.S. Geological Survey (USGS) for teleseismic events with moment magnitude (Mw) larger or equal to 5.5 between October 8, 2005, and October 17, 2008. A total of 389 events were found and their source parameters are listed in Table 2. A map showing the geographic distribution of the source events within the year of October 2005–October 2008 is shown in Figure 3.

Three-component broadband data for each of the selected events were collected from the CNSN Data Center (http://www.earthquakescanada.nrcan.gc.ca/stndon/index-eng.php). For each record, the mean and trend were first removed. Then the two horizontal components were rotated to radial and transverse directions according to the great circle path defined by the locations of source event and station.

We followed the iterative time-domain deconvolution method of Ligorria and Ammon (1999) to calculate the receiver functions of each station-event pair. The radial and transverse components of receiver function were derived by deconvolving the vertical component of the ground motion from the radial and transverse components, respectively. The calculation of receiver functions was performed for all stations in the GSL region, including CNSN permanent broadband stations.

In general, the receiver function is representative of local velocity structure directly beneath the recording station. Due to the steep incident angles of teleseismic body waves (~60°), the corresponding lateral extent is ~20 km at the depth of continental Moho discontinuity. A key advantage of receiver function analysis is that it is very sensitive to velocity reversals and the existence of low velocity zones, which are very difficult to be delineated from conventional seismic refraction or reflection profiling.

Many of the collected teleseismic events did not generate high-quality receiver functions suitable for velocity structure inversion, probably due to the combined effects of high background microseismic noise (from natural phenomena, such as severe weather conditions over the Atlantic Ocean and Gulf of St. Lawrence) and relatively poor site conditions at non-bedrock sites . In Figures 4–15, we show the selected long-period receiver functions (water-filling parameter A=2) as a function of back azimuth for all stations. The short-period version (water-filling parameter A=5) is shown in Figures 16–27.

4. Preliminary Inversion Results

In this section, we present the preliminary results of receiver function inversion for the crustal structure beneath broadband seismograph stations of the Atlantic array. The Neighborhood Algorithm is used in the inversion to estimate the thickness and velocities of horizontal layers from the short-period (A=5) radial component of the receiver function (Sambridge, 1999a and 1999b). Such a method has been successfully applied to the Haida Gwaii region to study the complicated underthrusting structure along the predominantly strike-slip Queen Charlotte fault system (Bustin et al., 2007). In this study, the inversion for dipping structures has been attempted, but no satisfactory results have been obtained to date. We suspect that the limited back-azimuth range of the high-quality receiver functions and the relatively short deployment period are the main reasons for the lack of solution.

Reasonable inversion results were obtained for 3 temporary stations (BATG, MALG, and NATG) and 3 permanent stations (DRLN, ICQ, and LMN). We were unsuccessful in delineating the crustal structures beneath other temporary stations because either the corresponding receiver functions do not show clear signals of P-to-S conversion or the converted phases from different back azimuths are too incoherent to warrant good inversion results. For these stations, it is probably necessary to take a different approach to constrain the local crustal structures. Further discussion of this issue will be given in Section 5.

4.1 Station BATG

Figure 28 shows the inversion result of station BATG. The Moho signature is clearly evident at ~3.9 s while significant negative amplitudes are observed at 0.5 s and 2.2 s, respectively. These large negative amplitudes imply the existence of low-velocity layers in the crust. Indeed, the inversion result shows two large velocity decreases at the depths of 5 and 18 km, respectively. The Moho depth is estimated to be 28 km.

4.2 Station DRLN

Figure 29 shows the inversion result of station DRLN. Similar to BATG, the Moho phase is clearly observed at ~4 s, but the receiver function waveform between the P and Moho phases is much less complicated with no negative amplitudes except immediately before the Moho phase. The inversion result shows a low-velocity layer immediately above the Moho discontinuity, suggesting the existence of a low-velocity lower crust. The top sedimentary layer has a thickness of 5.5 km, whereas the Moho depth is estimated at 29 km.

4.3 Station ICQ

Figure 30 shows the inversion result of station ICQ. Unlike stations BATG and DRLN, this station has a much thicker crust (44 km), which is evident from the much later arrival of the Moho phase (~5.2 s). There are a number of small amplitudes between the P and Moho phases with both positive and negative polarities. These phases correspond to small velocity contrasts within the crust, and may hint at the existence of low-velocity layers at various depths.

4.4 Station LMN

Figure 31 shows the inversion result of station LMN. The Moho depth is well constrained at 40 km by the clear Ps converted phase arriving at 4.6 s. There is a small negative amplitude near 1 s, suggesting a low-velocity layer between the depths of 8 and 15 km.

4.5 Station MALG

Figure 32 shows the inversion result of station MALG. This station appears to have a very thick sedimentary layer (~9 km) with a low Vs (3.0 km/s). The existence of a mid-crust low-velocity layer is also suggested by a pair of negative and positive amplitudes arriving at 2.1 s and 3.5 s, respectively. The crustal thickness is well constrained at 37 km by the Moho phase arriving at 5 s.

4.6 Station NATG

Figure 33 shows the inversion result of station NATG. This station has the thickest crust in the GSL region. The Moho phase arrives at 5.3 s, corresponding to a depth of 46 km. Similar to station ICQ, there are a series of phase arrivals, with both positive and negative polarities, between the P and Moho phases, implying the existence of a sequence of velocity layers. However, the amplitudes are generally smaller, meaning that the corresponding velocity contrasts are not as prominent as those beneath ICQ.

5. Interpretation and Conclusions

A schematic interpretation of our preliminary receiver function inversion results is shown in Figure 34. The north–south profile along approximately the 65°W meridian is shown at the top panel and the east–west profile along approximately the 49.5°N is at the bottom.

For the N–S profile, the shallow structure shows a clear dipping trend toward the south. The crustal thickness, however, varies significantly from 28 km at the middle (BATG) to 40 km in the south (LMN) and 44 km in the north (ICQ). A low-velocity layer is observed at the mid-crust in the north (ICQ) and lower crust in the middle (BATG), but not in the south (LMN).

For the E–W profile, the thickest crust is found at the middle beneath NATG (46 km) and the thickness gradually decreases to the east (31 km, DRLN) and slightly to the west (44 km, ICQ). The lower crust appears to correspond to a low-velocity layer with varying thickness (~13 km beneath NATG to 6 km beneath ICQ and DRLN).

It is noticeable that many of the 10 temporary stations of the Atlantic array do not have sufficient high-quality receiver functions for us to perform velocity model inversion, despite the large number of teleseismic events listed in Table 2. Given the relatively noisy site conditions, a high-quality receiver function would require the source event to be much larger or many source events such that the random noise can be reduced through stacking. Therefore, we recommend that future deployments in this region should probably utilize sub-surface sensors to minimize as much background noise as possible. The deployment durations should also be increased to collect as numerous events with varied azimuth coverage as possible.

Alternatively, it is suggested that the detailed crustal structure of the GSL region can be investigated using the ambient seismic noise as the source (e.g., Benson et al., 2007). This technique, known as ambient seismic noise tomography, does not depend on the distribution and size of natural earthquakes and could be combined with the receiver function analysis to give a more complete velocity image of the study region. Such an analysis could be done with the data recorded in this deployment.

Acknowledgement

We are grateful to the POLARIS consortium and the CNSN for providing the seismic data. We thank Maurice Lamontagne for conducting a critical review of this report, Julie Halliday, Hyun-seung Kim, and Patrick Potter for their assistance during various stages of this study. Patrick Potter, Issam Al-Khoubbi, and Calvin Andrew are greatly appreciated for their assistance during the deployment of the temporary seismic network. This study was supported by the Geological Survey of Canada through the Secure Canadian Energy Supply, Offshore Geoscience, and Geoscience for New Energy Supply programs.

References

Bensen, G. D., M. H. Ritzwoller, M. P. Barmin, A. L. Levshin, F. Lin, M. P. Moschetti, N. M. Shapiro, and Y. Yang (2007), Processing seismic ambient noise data to obtain reliable broad-band surface wave dispersion measurements, *Geophys. J. Int., 169*, 1239-1260, doi: 10.1111/j.1365-246X.2007.03374.x.

Bustin, A. M. M., R. D. Hyndman, H. Kao, and J. F. Cassidy (2007), Evidence for underthrusting beneath the Queen Charlotte Margin, British Columbia, from teleseismic receiver function analysis, *Geophys. J. Int., 171*, 1198-1211.

Chian, D., F. Marillier, J. Hall, and G. Quinlan (1998), An improved velocity model for the crust and upper mantle along the central mobile belt of the Newfoundland Appalachian orogen and its offshore extension, *Can. J. Earth Sci., 35 (11)*, 1238-1251.

Funck, T., H. R. Jackson, K. E. Louden, S. A. Dehler, and Y. Wu (2004), Crustal structure of the northern Nova Scotia rifted continental margin (Eastern Canada), *J. Geophys. Res., 109*, B09102, doi:10.1029/2004JB003008.

Hall, J., F. Marillier, and S. Dehler (1998), Geophysical studies of the structure of the Appalachian orogen in the Atlantic borderlands of Canada, *Can. J. Earth Sci., 35 (11)*, 1205-1221.

Hughes, S., J. Hall, and J.H. Luetgert (1994), The seismic velocity structure of the Newfoundland Appalachian orogen, *J. Geophys. Res., 99*, 13,633-13,653.

Jackson, H.R. (2002), Seismic refraction profiles in the Gulf of Saint Lawrence and implications for extent of continuous Grenville lower crust, *Can J. Earth Sci., 39 (1)*, 1-17.

Jackson, H.R., Marillier, F., and J. Hall (1998), Seismic refraction data in the Gulf of Saint Lawrence: implications for the lower-crustal blocks, *Can J. Earth Sci., 35(11)*, 1222-1237.

Ligorria, J. P., and C. J. Ammon (1999), Iterative deconvolution and receiver-function estimation, *Bull. Seismol. Soc. Am., 89(5),* 1395-1400.

Marillier, F., and J. Verhoef (1989), Crustal thickness under the Gulf of St. Lawrence, northern Appalachians, from gravity and deep seismic data, *Can J. Earth Sci., 26 (8)*, 1517-1532.

Marillier, F., M. Dentith, K. Michel, I. Reid, B. Roberts, J. Hall, J. Wright, K. Louden, P. Morel-a-l'Huissier, and C. Spencer (1991), Coincident seismic-wave velocity and reflectivity properties of the lower crust beneath the Appalachian Front, west of Newfoundland, *Can. J. Earth Sci., 28 (1)*, 94-101.

Marillier, F., J. Hall, S. Hughes, K. Louden, I. Reid, B. Roberts, R. Clowes, T. Coté, J. Fowler, S. Guest, H. Lu, J. Luetgert, G. Quinlan, C. Spencer, and J. Wright (1994), Lithoprobe East onshore-offshore seismic refraction survey – constraints on interpretation of reflection data in the Newfoundland Appalachians, *Tectonophysics, 232*, 43-58.

Quinlan G.M., J. Hall, H. Williams, J.A. Wright, S.P. Colman-Sadd, S.J. O'Brien, G.S. Stockmal, and F. Marillier (1992), Lithoprobe onshore seismic reflection transects across the Newfoundland Appalachians, *Can. J. Earth Sci., 29 (9)*, 1865-1877.

Sambridge, M. (1999a), Geophysical inversion with a neighbourhood algorithm - I. Searching a parameter space, *Geophys. J. Int., 138*, 479-494.

Sambridge, M. (1999b), Geophysical Inversion with a Neighbourhood Algorithm -II. Appraising the ensemble, *Geophys. J. Int., 138*, 727-746.

Williams, H., S.A. Dehler, A.C. Grant, and G. N. Oakey (1999), Tectonics of Atlantic Canada, *Geosci. Canada, 26 (2)*, 51-70.

Table 1. Configuration of the Atlantic array

Station Code	Location	Latitude (°N)	Longitude (°E)	Elevation (km)	Start date (yyyymmdd)	End date (yyyymmdd)	Power
BATG	Bathurst, NB	47.27666	-66.05989	0.336	20051022	Active (as of 20130701)	AC
CHEG	Cheticamp, NS	46.80836	-60.67447	0.4459	20051019	Active (as of 20130701)	AC
CODG	Codroy, NL	47.84056	-59.25352	0.05	20051006	20080910	Solar Panels
GASG	Gaspe, QC	48.94626	-66.11613	0.2606	20051025	20081021	Solar Panels
GBN	Guysborough, NS	45.40774	-61.51284	0.038	20051017	Active (as of 20130701)	AC
MADG	Magdelan Islands, QC	47.27478	-61.68917	0.078	20051001	20081015	Solar Panels
MALG	Malagash, NS	45.79035	-63.32714	0.022	20051015	20081009	AC
NATG	Baie Johan Beetz, QC	50.28721	-62.81015	-0.0018	20051126	Active (as of 20130701)	AC
SABG	Sable Island, NS	43.93124	-60.00843	0	20051013	20090429	AC
TIGG	Tignish, PE	47.00153	-63.99805	0.008	20050929	20071105	Solar Panels

Table 2. Source parameters of teleseismic events during the study time period. (Extracted from USGS earthquake catalogue)

Origin time	Lat.	Lon.	Mw	Depth	Location
2005 10 08 03:50:40	34.493N	73.629E	M7.6	26.0km	Pakistan
2005 10 15 15:51:07	23.321N	123.356E	M6.5	183.0km	NE of Taiwan
2005 10 19 11:44:43	36.383N	140.833E	M6.4	41.5km	Honshu, Japan
2005 11 14 21:38:51	38.101N	144.925E	M7.0	11.0km	Honshu, Japan
2005 11 17 19:26:56	22.263S	67.784W	M6.9	162.5km	Potosi, Bolivia
2005 11 19 14:10:14	2.220N	96.763E	M6.5	30.0km	Simeulue, Indonesia
2005 11 27 10:22:19	26.784N	55.847E	M6.0	10.0km	Southern Iran
2005 12 02 13:13:09	38.122N	142.118E	M6.5	29.0km	Honshu, Japan
2005 12 05 12:19:57	6.174S	29.717E	M6.8	22.0km	Congo Tanzania
2005 12 11 14:20:43	6.594S	152.208E	M6.6	10.0km	Papua New Guinea
2005 12 12 21:47:46	36.332N	71.130E	M6.6	225.4km	Afghanistan
2005 12 13 03:16:06	15.265S	178.571W	M6.7	10.0km	Fiji
2006 01 02 06:10:49	60.807S	21.474W	M7.4	10.0km	South Sandwich
2006 01 02 22:13:40	19.926S	178.178W	M7.2	583.0km	Fiji
2006 01 04 08:32:31	28.077N	112.096W	M6.6	14.0km	Gulf of California
2006 01 08 11:34:55	36.300N	23.358E	M6.8	66.0km	Southern Greece
2006 01 27 16:58:53	5.482S	128.093E	M7.6	397.0km	Banda Sea
2006 02 02 12:48:43	17.747S	178.390W	M7.2	583.0km	Fiji
2006 02 22 22:19:07	21.259S	33.480E	M7.0	11.0km	Mozambique
2006 02 26 03:08:27	23.623S	179.961W	M6.4	535.8km	South of Fiji
2006 02 28 07:31:03	28.120N	56.865E	M6.0	18.0km	Southern Iran
2006 03 03 23:11:34	59.780N	153.040W	M5.0	99.2km	Southern Alaska
2006 03 04 00:53:31	0.862N	27.993W	M5.6	10.0km	Central MAR
2006 03 04 08:11:37	12.589N	89.368W	M5.7	27.8km	Off El Salvador
2006 03 05 10:42:15	64.949N	129.128W	M5.6	5.7km	Northwest Territories
2006 03 06 18:13:09	40.112S	78.529E	M6.2	10.0km	Mid Indian Ridge
2006 03 07 06:28:55	14.803S	167.380E	M6.2	136.2km	Vanuatu

```
2006 03 09 17:55:55   0.665N  26.101W M5.6  10.0km Central MAR
2006 03 14 06:57:33   3.593S 127.211E M6.7  30.6km Seram, Indonesia
2006 03 25 07:28:58  27.574N  55.685E M5.9  18.0km Southern Iran
2006 03 31 01:17:01  33.581N  48.794E M6.1   7.0km Western Iran
2006 03 31 13:21:00  29.609S 176.825W M6.5  17.0km Kermadec Islands

2006 04 01 10:02:20  22.868N 121.278E M6.2   9.0km Taiwan
2006 04 20 23:25:02  61.075N 167.085E M7.6  22.0km Koryakia, russia
2006 04 29 16:58:06  60.491N 167.516E M6.6  11.0km Koryakia, russia
2006 04 30 19:17:17  27.013S  70.959W M6.7  27.0km Chile
2006 04 30 21:40:58  27.211S  71.056W M6.5  12.0km Chile

2006 05 03 15:26:39  20.130S 174.164W M7.9  55.0km Tonga
2006 05 16 10:39:24  31.527S 179.303W M7.4 151.6km Kermadec Islands
2006 05 16 15:28:26   0.081N  97.073E M6.8  16.2km Nias region, Indonesia
2006 05 22 11:12:00  60.770N 165.735E M6.6  17.0km Koryakia, russia
2006 05 26 22:53:58   7.962S 110.458E M6.3  10.0km Java, Indonesia
2006 05 28 03:12:09   5.724S 151.133E M6.5  34.0km New Britain, Papua New Guinea

2006 06 11 20:01:29  33.290N 131.182E M6.3 154.8km Kyushu, Japan

2006 07 08 20:40:01  51.214N 179.312W M6.6  22.0km Andreanof Islands, Alaska
2006 07 17 08:19:28   9.222S 107.320E M7.7  34.0km S of Java, Indonesia

2006 08 07 22:18:54  15.777S 167.799E M6.8 141.0km Vanuatu
2006 08 11 14:30:39  18.492N 100.935W M6.1  60.1km Guerrero, Mexico
2006 08 20 03:41:47  61.006S  34.391W M7.0  10.0km Scotia Sea
2006 08 24 21:50:37  51.148N 157.522E M6.5  43.0km Kamchatka
2006 08 25 00:44:46  24.405S  67.028W M6.6 184.0km Salta, Argentina

2006 09 01 10:18:52   6.822S 155.535E M6.8  45.7km Papua New Guinea
2006 09 09 04:13:12   7.208S 120.087E M6.3 570.7km Flores Sea (Indon)
2006 09 10 14:56:07  26.331N  86.577W M6.0  10.0km Gulf of Mexico
2006 09 12 13:30:57  28.793S  68.644W M6.0 123.8km La Rioja, Argentina
2006 09 16 09:45:23   3.092S 129.506E M6.3  10.0km Seram, Indonesia
2006 09 17 09:34:10  31.668S  67.002W M6.2 105.2km San Juan, Argentina
2006 09 21 18:54:50   9.04S  110.37E  M6.0  25.0km South of Java, Indonesia
2006 09 22 02:32:25  26.78S   63.08W  M6.0 598.0km Santiago del Estero, Argentina
2006 09 28 01:36:48  46.50N  153.32E  M5.9  11.0km Kuril Islands
2006 09 28 06:22:09  16.56S  172.06W  M6.9  28.0km Samoa Islands region
2006 09 29 13:08:25  10.88N   61.75W  M6.1  53.0km Trinidad region
2006 09 29 18:23:05  10.81N   61.66W  M5.5  51.0km Trinidad region
2006 09 30 12:47:22   7.30N   34.63W  M5.5  10.0km Central MAR
2006 09 30 16:26:56  15.56S   73.14W  M6.0 107.0km Southern Peru
2006 09 30 17:50:23  46.36N  153.15E  M6.6  11.0km Kuril Islands
2006 09 30 17:56:16  46.19N  153.16E  M6.0  10.0km Kuril Islands

2006 10 01 09:06:02  46.47N  153.23E  M6.6  19.0km Kuril Islands
2006 10 03 18:03:14  18.85S  168.96E  M6.3 171.0km Vanuatu
2006 10 09 10:01:46  20.66N  120.03E  M6.3  10.0km Philippine Islands region
2006 10 09 11:08:28  20.70N  119.94E  M5.9  10.0km Philippine Islands region
2006 10 10 08:02:52  56.08S  122.39W  M6.0  10.0km Southern East Pacific Rise
2006 10 10 23:58:07  37.23N  142.71E  M6.0  30.0km East of Honshu, Japan
2006 10 11 06:00:48   8.44N  103.12W  M5.8  10.0km Northern East Pacific Rise
2006 10 12 18:05:56  31.256S  71.390W M6.4  29.3km Coquimbo, Chile
2006 10 13 13:47:40  46.311N 153.273E M6.3   8.8km Kuril Islands
2006 10 15 17:07:48  19.801N 156.053W M6.7  29.0km Hawaii region, Hawaii
2006 10 15 17:14:12  20.129N 155.983W M6.0  18.9km Hawaii region, Hawaii
2006 10 17 01:25:13   5.846S 151.010E M6.7  32.0km New Britain, Papua New Guinea
2006 10 18 10:45:33  15.086S 167.249E M6.3 115.0km Vanuatu
2006 10 20 10:48:58  13.427S  76.572W M6.5  33.1km Near coast, central Peru
2006 10 22 08:55:17  45.789S  96.039E M6.0  10.0km SE Indian ridge
2006 10 23 21:17:25  29.360N 140.272E M6.4  39.5km Izu Islands, Japan region
2006 10 24 03:03:52   4.954N 125.300E M6.1  56.6km Kepuluaun Sangihe, Indonesia
2006 10 26 22:54:32  13.39S   76.64W  M6.0  26.4km Near coast of central Peru

2006 11 06 20:56:51   5.415S 146.620E M6.0 134.0km Eastern New Guinea, Papua NG
2006 11 07 17:38:33   6.460S 151.170E M6.5  10.0km New Britain, Papua New Guinea
2006 11 12 18:21:25   6.200S 151.010E M6.2  12.0km New Britain, Papua New Guinea
2006 11 13 01:26:33  26.036S  63.244W M6.8 547.0km Santiago del Estero, Argentina
2006 11 13 16:12:28   6.386S 151.220E M6.2  11.0km New Britain, Papua New Guinea
2006 11 14 14:21:01   6.400S 127.980E M6.1 352.0km Banda Sea
2006 11 15 11:14:16  46.560N 153.250E M8.3  30.0km Kuril Islands
2006 11 15 11:25:08  47.220N 152.690E M5.9  10.0km Kuril Islands
2006 11 15 11:28:38  46.110N 154.100E M6.0  10.0km East of Kuril Islands
2006 11 15 11:29:22  46.370N 154.430E M6.2  10.0km East of Kuril Islands
```

2006 11 15	11:34:58	46.660N	155.310E	M6.5	10.0km	East of Kuril Islands
2006 11 15	11:40:55	46.480N	154.720E	M6.4	10.0km	East of Kuril Islands
2006 11 15	12:16:44	46.190N	154.660E	M5.9	10.0km	East of Kuril Islands
2006 11 15	21:22:23	46.340N	154.090E	M6.2	23.0km	Kuril Islands
2006 11 16	20:29:55	51.990S	139.130E	M6.1	10.0km	W Indian Antarctic ridge
2006 11 17	18:03:14	28.560N	129.910E	M6.2	35.0km	Ryukyu Islands, Japan
2006 11 19	18:57:33	4.490S	104.750W	M6.0	10.0km	Central East Pacific Rise
2006 11 29	01:32:20	2.549N	128.281E	M6.2	50.3km	Halmahera, Indonesia
2006 11 29	04:11:36	26.100N	44.740W	M4.8	10.0km	Northern mid Atlantic ridge
2006 11 29	15:22:24	53.740N	35.390W	M4.8	10.0km	Reykjanes ridge
2006 11 29	15:38:43	53.660N	35.300W	M5.6	10.0km	Reykjanes ridge
2006 11 30	11:33:17	21.320S	174.690W	M6.0	17.0km	Tonga
2006 11 30	21:20:11	53.990S	133.870W	M6.2	10.0km	Pacific Antarctic ridge
2006 12 01	03:58:22	3.487N	99.042E	M6.3	202.7km	Northern Sumatra, Indonesia
2006 12 01	14:01:49	8.225S	118.780E	M6.3	48.0km	Sumbawa region, Indonesia
2006 12 03	08:19:51	0.590S	19.720W	M5.6	10.0km	Central mid Atlantic ridge
2006 12 03	20:52:15	13.970N	91.260W	M5.9	55.0km	Guatemala
2006 12 07	19:10:20	46.230N	154.306E	M6.3	2.2km	East of Kuril Islands
2006 12 12	15:48:03	3.732N	124.680E	M6.3	213.7km	Celebes Sea
2006 12 22	19:50:48	10.681N	92.390E	M6.3	45.0km	Andaman Islands, India region
2006 12 26	12:26:22	21.818N	120.534E	M7.1	10.0km	Taiwan region
2006 12 26	12:34:14	22.023N	120.871E	M7.0	10.0km	Taiwan
2006 12 27	20:15:40	5.753S	154.470E	M6.0	369.9km	Papua New Guinea region
2006 12 30	08:30:49	13.336N	51.434E	M6.3	10.0km	Gulf of Aden
2007 01 08	12:48:40	8.090N	92.450E	M6.1	11.0km	Nicobar Islands, India region
2007 01 08	17:21:50	39.810N	70.320E	M6.0	17.0km	Kyrgyzstan
2007 01 08	20:52:20	18.590S	177.850W	M6.3	407.0km	Fiji region
2007 01 11	14:31:20	3.640S	127.300E	M6.0	13.0km	Seram, Indonesia
2007 01 13	04:23:20	46.270N	154.450E	M8.1	10.0km	East of the Kuril Islands
2007 01 13	17:37:06	46.900N	156.250E	M6.0	10.0km	East of the Kuril Islands
2007 01 17	04:28:26	3.330S	139.880E	M6.0	104.0km	Papua, Indonesia
2007 01 17	23:18:50	10.140N	58.710E	M6.2	10.0km	Carlsberg Ridge
2007 01 20	06:21:04	55.110S	29.350W	M6.2	10.0km	South Sandwich Islands region
2007 01 21	11:27:45	1.060N	126.300E	M7.5	22.0km	Molucca Sea
2007 01 21	17:32:55	1.060N	126.330E	M6.2	23.0km	Molucca Sea
2007 01 25	10:59:18	22.570N	121.930E	M6.0	39.0km	Taiwan region
2007 01 30	04:54:50	54.888S	145.733E	M6.8	10.0km	West of Macquarie Island
2007 01 30	21:37:50	20.983N	144.797E	M6.6	59.3km	Northern Mariana Islands
2007 01 31	03:15:56	29.593S	177.935W	M6.5	53.7km	Kermadec Islands, NZ
2007 02 04	03:33:19	35.258N	35.984W	M5.6	10.0km	Northern Mid Atlantic Ridge
2007 02 04	20:56:59	19.480N	78.306W	M6.2	10.0km	Cuba region
2007 02 04	21:17:53	56.153S	122.990W	M6.1	10.0km	Southern East Pacific Rise
2007 02 08	10:21:56	8.710N	39.400W	M5.2	10.0km	Central MAR
2007 02 08	12:05:35	8.750N	39.410W	M5.0	10.0km	Central MAR
2007 02 08	14:32:11	8.500N	39.260W	M5.1	10.0km	Central MAR
2007 02 08	16:28:07	8.660N	39.360W	M5.3	10.0km	Central MAR
2007 02 12	10:35:21	35.800N	10.290W	M6.0	10.0km	Azores Cape St.Vincent ridge
2007 02 12	12:45:32	5.590N	126.120E	M6.1	29.0km	Mindanao, Philippines
2007 02 17	00:02:58	41.907N	143.454E	M6.0	35.0km	Hokkaido, Japan region
2007 02 20	08:04:25	1.019S	127.013E	M6.7	11.0km	Kepulauan Obi, Indonesia
2007 02 24	02:36:23	7.011S	80.365W	M6.4	23.0km	Off coast of northern Peru
2007 02 28	23:13:20	55.174S	29.184W	M6.2	35.0km	South Sandwich Islands region
2007 03 01	23:11:52	26.599N	44.545W	M5.9	10.0km	Northern mid Atlantic Ridge
2007 03 06	03:49:39	0.510S	100.520E	M6.4	19.0km	Southern Sumatra, Indonesia
2007 03 06	05:49:28	0.490S	100.520E	M6.3	30.0km	Southern Sumatra, Indonesia
2007 03 08	05:03:31	29.920N	140.240E	M6.1	133.0km	Izu islands, Japan
2007 03 08	11:14:32	58.210S	7.640W	M6.2	10.0km	East of the South Sandwich Isl.
2007 03 09	03:22:42	43.210N	133.550E	M6.0	442.0km	Primor Ye, Russia
2007 03 10	17:03:38	74.175N	8.595E	M5.7	10.0km	Greenland Sea
2007 03 13	02:59:06	26.305N	110.515W	M6.0	42.0km	Gulf of California
2007 03 17	17:42:26	1.130N	126.180E	M6.2	35.0km	Molucca Sea
2007 03 17	22:43:09	4.550N	78.500W	M6.0	10.0km	South of Panama
2007 03 18	02:11:05	4.580N	78.510W	M6.2	8.0km	South of Panama
2007 03 25	00:40:02	20.660S	169.420E	M7.1	35.0km	Vanuatu
2007 03 25	00:41:57	37.310N	136.570E	M6.7	5.0km	near West coast Honshu, Japan
2007 03 25	01:08:19	20.780S	169.400E	M6.9	35.0km	Vanuatu
2007 03 31	12:49:04	56.070S	123.251W	M6.2	10.0km	South East Pacific Rise
2007 04 01	20:39:56	8.481S	156.978E	M8.1	10.0km	Solomon Islands
2007 04 01	20:47:32	7.133S	155.661E	M6.7	10.0km	Solomon Islands
2007 04 01	21:11:34	7.441S	155.774E	M6.4	10.0km	Solomon Islands
2007 04 01	21:15:23	7.336S	155.658E	M6.0	10.0km	Solomon Islands

```
2007 04 02 10:49:15   7.197S 156.192E M6.0  10.0km Solomon Islands
2007 04 02 12:02:23   8.539S 157.548E M6.2  10.0km Solomon Islands
2007 04 02 23:20:23   8.494S 157.352E M6.2  10.0km Solomon Islands
2007 04 03 03:35:07  36.528N  70.668E M6.2 210.5km Hindu Kush, Afghanistan
2007 04 03 12:04:28   7.844S 155.805E M6.0  10.0km Solomon Islands
2007 04 03 20:26:15  20.695S 168.864E M6.2  41.4km Loyalty Islands
2007 04 04 00:39:45   7.121S 156.073E M6.0  10.0km Solomon Islands
2007 04 04 06:34:35   7.774S 156.489E M6.4  10.0km Solomon Islands
2007 04 04 11:00:27  20.754S 168.880E M6.2  10.0km Loyalty Islands
2007 04 04 11:02:29  20.727S 169.028E M6.4  10.0km Vanuatu
2007 04 05 03:56:51  37.343N  24.613W M6.3  14.0km Azores Islands region
2007 04 07 07:09:26  37.344N  24.506W M6.3  10.0km Azores Islands region
2007 04 07 09:51:52   2.924N  95.699E M6.1  30.0km Simeulue, Indonesia

2007 04 12 18:24:48  61.846S 160.663E M6.0   1.3km Balleny Islands region
2007 04 13 05:42:23  17.318N 100.122W M6.0  34.0km Guerrero, Mexico
2007 04 13 18:24:19  35.062S 108.864W M6.1  10.0km Southern East Pacific Rise
2007 04 16 13:20:38  57.953S 147.637E M6.4  10.0km West of Macquarie Island

2007 04 20 00:26:41  25.733N 125.140E M6.1  10.0km SW Ryukyu Islands, Japan
2007 04 20 01:45:56  25.697N 125.191E M6.3   9.0km SW Ryukyu Islands, Japan
2007 04 21 07:12:47   3.559S 151.326E M6.1 401.7km New Ireland region, Papua
2007 04 21 17:20:32  13.911S 166.881E M6.0  40.7km Vanuatu
2007 04 21 17:53:47  45.274S  72.604W M6.2  44.1km Aisen, Chile
2007 04 25 13:34:16  14.298S 166.819E M6.3  69.3km Vanuatu

2007 05 04 12:06:52   1.440S  14.920W M6.2  10.0km North of Ascension Island
2007 05 05 08:51:39  34.230N  81.930E M6.0   9.0km Western Xizang
2007 05 06 21:11:52  19.400S 179.330W M6.5 676.0km Fiji region
2007 05 06 22:01:08  19.390S 179.340W M6.1 688.0km Fiji region
2007 05 07 11:15:16  44.830S  80.490W M6.1   4.0km Off coast of Aisen, Chile
2007 05 16 08:56:16  20.510N 100.740E M6.3  23.0km Laos
2007 05 23 19:09:15  22.020N  96.260W M5.6  10.0km Gulf of Mexico
2007 05 25 17:47:31  24.180S  67.001W M5.9 180.2km Salta, Argentina
2007 05 29 01:03:28   4.622S 151.865E M6.1 128.1km New Britain region, PNG
2007 05 29 09:36:04   1.137S 127.408E M6.1  10.0km Kepulauan Obi, Indonesia
2007 05 30 20:22:13  52.144N 157.313E M6.4 115.8km Kamchatka pen., Russia

2007 06 02 21:34:58  23.015N 101.071E M6.2  10.0km Yunnan, China
2007 06 07 00:40:41   3.377S 146.763E M6.2  22.6km Bismarck Sea
2007 06 13 19:29:41  13.616N  90.816W M6.7  23.0km Offshore Guatemala
2007 06 14 17:41:06   5.701S 151.596E M6.0  57.8km New Britain region, PNG
2007 06 18 06:18:46   3.573S 151.010E M6.3  10.0km New Ireland region, PNG
2007 06 24 00:25:18  55.574S   2.763W M6.5  10.0km Southern MAR
2007 06 26 22:23:03  10.490S 108.144E M6.0  10.0km South of Java, Indonesia
2007 06 28 02:52:09   7.938S 154.616E M6.7  10.0km Bougainville region, PNG

2007 07 03 08:26:01   0.742N  30.244W M6.3  10.0km Central MAR
2007 07 06 01:09:21  16.580N  93.550W M6.0 143.0km Chiapas, Mexico
2007 07 12 05:23:49   7.920S  74.340W M6.1 152.0km Northern Peru
2007 07 13 21:54:43  51.813N 176.234W M6.0  35.0km Aleutian Islands, Alaska
2007 07 15 09:27:35  15.373S 168.565E M6.1   8.0km Vanuatu
2007 07 15 13:08:01  52.620N 168.042W M6.1  10.0km Aleutian Islands, Alaska
2007 07 15 13:26:15  52.378N 168.040W M5.8  10.0km Aleutian Islands, Alaska
2007 07 16 01:13:23  37.576N 138.469E M6.6  10.0km West coast Honshu, Japan
2007 07 16 14:17:37  36.788N 134.897E M6.8 349.0km Sea of Japan
2007 07 17 09:39:35  26.135S 177.769W M6.1  54.9km South of Fiji Islands
2007 07 18 00:07:36  26.210S 177.746W M6.1  10.0km South of Fiji Islands
2007 07 21 13:27:04   7.976S  71.130W M6.1 632.9km Amazonas, Brazil
2007 07 21 15:34:52  22.270S  65.752W M6.2 289.6km Jujuy, Argentina
2007 07 25 23:37:31   7.150N  92.490E M6.1  15.0km Nicobar Islands, India
2007 07 26 05:40:16   2.820N 127.480E M6.9  25.0km Molucca Sea
2007 07 31 22:55:31   0.095S  17.800W M6.1  10.0km N of Ascension Island

2007 08 01 17:08:51  15.736S 167.745E M7.2 120.0km Vanuatu
2007 08 02 02:37:43  47.259N 141.750E M6.2   5.0km Tatar Strait, Russia
2007 08 02 03:21:46  51.340N 179.944W M6.7  46.7km Andreanof Islands, Alaska
2007 08 04 14:24:58   4.483S 105.178W M6.0  39.2km Central East Pacific Rise
2007 08 05 09:28:42  19.161S 168.720E M6.0  59.7km Vanuatu
2007 08 08 17:04:58   5.968S 107.655E M7.5 289.2km Java, Indonesia
2007 08 12 12:05:20  11.376S 166.274E M6.0  42.0km Santa Cruz Islands
2007 08 13 10:27:28  60.368S 152.858E M6.1  26.3km West of Macquarie I
2007 08 15 20:22:14  50.568N 177.507W M6.5  21.1km Andreanof Islands, Alaska
2007 08 15 23:40:57  13.358S  76.522W M8.0  30.2km Near coast of Central Peru
2007 08 16 05:16:58  14.250S  76.061W M6.3  35.0km Near coast of central Peru
2007 08 16 08:39:27   9.715S 159.335E M6.7   1.8km Solomon Islands
```

```
2007 08 16 11:35:30  14.395S  76.154W M6.0  35.0km Near coast of central Peru
2007 08 17 03:04:03   5.272S 129.513E M6.2  10.0km Banda Sea
2007 08 18 12:32:20  22.192S 174.716E M6.0  35.0km Southeast of Loyalty Is.
2007 08 20 12:37:06   0.210S  18.160W M5.7  10.0km Central MAR
2007 08 20 13:46:17   6.120N 127.410E M6.4   8.0km Philippine I region
2007 08 20 22:42:29   8.020N  39.270W M6.5  10.0km Central MAR
2007 08 26 12:37:31  17.330S 174.400W M6.1 127.0km Tonga

2007 09 01 01:56:49  27.792N  44.039W M5.6  10.0km Northern MAR
2007 09 01 19:14:22  24.821N 109.704W M6.1  10.0km Gulf of California
2007 09 02 01:05:19  11.510S 165.814E M7.2  35.0km Santa Cruz Islands
2007 09 03 16:14:54  45.795N 150.051E M6.2  96.5km Kuril Islands
2007 09 06 17:51:27  24.334N 122.324E M6.5  62.9km Taiwan region
2007 09 10 01:49:11   2.945N  78.069W M6.8  10.0km Near W coast Colombia
2007 09 12 11:10:26   4.521S 101.370E M8.4  30.0km Southern Sumatra, Indonesia
2007 09 12 14:40:01   3.227S 101.358E M6.0  10.0km Southern Sumatra, Indonesia
2007 09 12 23:49:01   2.526S 100.964E M7.8  10.0km Kepulauan Mentawai, Indonesia
2007 09 13 03:35:27   2.223S  99.564E M7.1  10.0km Kepulauan Mentawai, Indonesia
2007 09 13 09:48:44   3.794N 126.411E M6.2  21.9km Kepulauan Talaud, Indonesia
2007 09 13 16:09:10   3.247S 101.439E M6.2   3.3km Southern Sumatra, Indonesia
2007 09 14 06:01:32   4.108S 101.150E M6.2  23.0km Southern Sumatra, Indonesia
2007 09 19 07:27:50   2.720S 100.970E M6.0  35.0km Kepulauan Mentawai, Indonesia
2007 09 20 08:31:14   2.020S 100.130E M6.7  30.0km Kepulauan Mentawai, Indonesia
2007 09 25 05:16:00  30.960S 179.880E M6.2 408.0km Kermadec Islands region
2007 09 26 12:36:23   4.880S 153.400E M6.7  10.0km New Ireland region, PNG
2007 09 26 15:43:01   1.740S  99.510E M6.0  26.0km Kepulauan Mentawai, Indonesia
2007 09 27 19:57:45  21.278S 169.366E M6.1  21.1km Southeast of Loyalty Islands
2007 09 28 01:01:48  21.347S 169.420E M6.3  10.0km Southeast of Loyalty Islands
2007 09 28 01:35:52  21.257S 169.440E M6.3  10.0km Southeast of Loyalty Islands
2007 09 28 13:38:58  21.980N 142.685E M7.4 261.3km Mariana Islands region
2007 09 30 02:08:29  10.487N 145.682E M6.9  10.0km South of the Mariana Islands
2007 09 30 05:23:34  49.418S 163.954E M7.4  10.0km Auckland Isl., New Zealand
2007 09 30 09:47:50  49.409S 163.265E M6.6  10.0km Auckland Isl., New Zealand

2007 10 02 03:43:41   4.360S 100.947E M6.2  35.0km SW of Sumatra, Indonesia
2007 10 02 18:00:08  54.581N 161.768W M6.3  47.9km Alaska peninsula
2007 10 04 12:40:31   2.545N  92.881E M6.2  30.0km Off W coast Northern Sumatra
2007 10 05 07:17:55  25.243S 179.414E M6.5 534.9km South of the Fiji Islands
2007 10 06 12:38:55  18.712N 147.153E M6.1  63.8km Mariana Islands region
2007 10 09 15:03:42   4.838S 152.849E M6.0  51.6km New Britain region, PNG
2007 10 10 00:19:17   1.730S  99.470E M6.0  26.0km Kepulauan Mentawai, Indonesia
2007 10 11 22:42:11  17.640N  46.490W M5.2  10.0km Northern MAR
2007 10 13 17:45:53  21.242S 169.200E M6.1  40.4km Southeast of Loyalty Islands
2007 10 15 12:29:37  44.713S 167.464E M6.8  25.4km South Island of New Zealand
2007 10 15 21:28:24  44.893S 167.531E M6.1  19.0km South Island of New Zealand
2007 10 16 21:05:48  25.617S 179.419E M6.6 549.6km South of the Fiji Islands
2007 10 18 16:13:14  30.101N  42.544W M5.5  10.0km Northern MAR
2007 10 21 10:24:52   6.325S 154.753E M6.0  46.9km Bougainville region, PNG
2007 10 24 21:02:51   3.870S 100.960E M6.8  20.0km Kepulauan Mentawai, Indonesia
2007 10 25 13:50:01  46.050N 154.110E M6.1   6.0km East of Kuril Islands
2007 10 31 03:30:20  18.900N 145.290E M7.2 223.0km Pagan region, N Mariana Is
2007 10 31 13:44:19  51.360N 178.400W M6.0  28.0km Andreanof Islands, Aleutian I.

2007 11 02 22:31:44  55.480S 128.810W M6.1  10.0km Pacific Antarctic ridge
2007 11 10 01:13:34  52.120S 159.560E M6.5  10.0km Macquarie Island region
2007 11 14 15:40:50  22.200S  69.860W M7.7  40.0km Antofagasta, Chile
2007 11 15 15:03:08  22.810S  70.310W M6.1  27.0km Offshore Antofagasta, Chile
2007 11 15 15:05:58  22.930S  70.270W M6.8  26.0km Antofagasta, Chile
2007 11 16 03:13:00   2.270S  77.800W M6.8 123.0km Peru Ecuador border region
2007 11 18 05:40:07  22.580S  66.170W M6.0 203.0km Jujuy, Argentina
2007 11 19 00:52:13  21.040S 178.740W M6.3 558.0km Fiji region
2007 11 19 20:32:48  43.541N 127.507W M5.7  10.0km off coast of Oregon
2007 11 20 12:52:59   6.807S 155.617E M6.0  50.8km Bougainville region, PNG
2007 11 20 17:55:53  22.848S  70.447W M6.1  23.5km Offshore Antofagasta, Chile
2007 11 22 08:48:31   5.843S 147.022E M6.7  77.5km Eastern New Guinea reg, PNG
2007 11 25 16:02:19   8.294S 118.360E M6.5  42.5km Sumbawa region, Indonesia
2007 11 25 17:41:37   2.235S 100.397E M6.0  30.0km Kepulauan Mentawai, Indonesia
2007 11 25 19:53:08   8.176S 118.497E M6.5  35.0km Sumbawa region, Indonesia
2007 11 27 11:49:58  10.990S 162.220E M6.6  16.0km Solomon Islands
2007 11 29 03:26:21  36.930S  97.290W M6.3  10.0km West Chile Rise
2007 11 29 19:00:19  14.970N  61.230W M7.4 147.0km Martinique Region

2007 12 09 07:28:21  25.872S 177.517W M7.8 149.2km South of Fiji Islands
2007 12 12 23:40:00  52.150N 131.480W M5.7  10.0km Queen Charlotte Is region
2007 12 13 05:20:26  23.163S  70.539W M6.0  41.2km Antofagasta, Chile
2007 12 13 07:23:47  23.013S  70.340W M6.2  58.7km Antofagasta, Chile
```

```
2007 12 13 15:51:29  15.178S 172.402W M6.2  33.0km Samoa Islands region
2007 12 15 08:03:15   7.530S 127.490E M6.0 177.0km Kepulauan Barat Daya, Indon.
2007 12 15 09:39:48   6.620S 131.170E M6.4  15.0km Kepulauan Tanimbar region
2007 12 16 08:09:19  22.910S  70.060W M6.7  58.0km Antofagasta, Chile
2007 12 19 09:30:31  51.495N 179.473W M7.2  56.3km Andreanof Is, Alaska
2007 12 20 07:55:19  38.842S 177.930E M6.6  35.6km North Island, New Zealand
2007 12 21 07:24:36  51.422N 179.075W M6.1  35.0km Andreanof Is, Alaska
2007 12 22 07:11:11   2.390S 139.086E M6.1  35.0km Near N coast, Papua, Indon.
2007 12 25 14:04:34  38.502N 141.969E M6.1  49.9km Near E coast, Honshu, Japan
2007 12 26 22:04:56  52.670N 168.230W M6.4  35.0km Fox Islands, Aleutian Is.

2008 01 01 18:55:04   5.970S 146.860E M6.3  79.0km E. New Guinea region, PNG
2008 01 04 07:29:18   2.780S 100.970E M6.0  35.0km Kepalauan Mentawai, Indonesia
2008 01 05 11:01:05  51.240N 130.770W M6.6  10.0km Queen Charlotte Is region
2008 01 05 11:44:48  51.140N 130.570W M6.4  10.0km Queen Charlotte Is region
2008 01 06 05:14:20  37.240N  22.680E M6.2  83.0km Southern Greece
2008 01 09 08:26:45  32.310N  85.200E M6.4  10.0km Western Xizang
2008 01 09 14:40:00  51.690N 131.130W M6.0  10.0km Queen Charlotte Is region
2008 01 10 01:37:18  43.840N 127.270W M6.3  10.0km Off coast of Oregon
2008 01 15 17:52:15  21.900S 179.520W M6.5 596.0km Fiji region
2008 01 20 20:26:06   2.348N 126.916E M6.1  41.9km Molucca Sea
2008 01 22 07:55:53  15.296S 175.320W M6.0  35.0km Tonga
2008 01 22 10:49:27  15.331S 175.664W M6.1  40.5km Tonga
2008 01 22 17:14:57   1.011N  97.436E M6.2  20.0km Nias region, Indonesia
2008 01 30 07:32:48   7.324S 127.753E M6.2  42.4km Kepulauan Barat Daya, Ind.

2008 02 01 12:10:08  21.380S 179.428W M6.0 623.2km Fiji region
2008 02 04 17:01:31  20.020S  69.839W M6.3  35.1km Tarapaca, Chile
2008 02 08 09:38:14  10.671N  41.899W M6.9   9.0km NORTHERN MID ATLANTIC RIDGE
2008 02 12 12:50:18  16.357N  94.304W M6.4  83.0km OAXACA, MEXICO
2008 02 14 10:09:22  36.501N  21.670W M6.9  29.0km SOUTHERN GREECE
2008 02 14 12:08:55  36.345N  21.863W M6.5  28.0km SOUTHERN GREECE
2008 02 20 18:27:06  36.288N  21.775W M6.1   9.9km SOUTHERN GREECE
2008 02 21 02:46:17  77.080N  18.573W M6.1  10.0km SVALBARD REGION
2008 02 21 14:16:02  41.153N 114.867W M6.0   6.7km NEVADA
2008 04 24 12:14:49   1.182N  23.471W M6.5  10.0km CENTRAL MID ATLANTIC RIDGE
2008 05 02 01:33:37  51.864N 177.528W M6.6  14.0km ANDREANOF ISLANDS, ALEUTIAN IS
2008 05 23 19:35:34   7.313N  34.897W M6.5   8.0km CENTRAL MID ATLANTIC RIDGE
2008 05 25 19:18:24  55.906N 153.508W M6.0  20.0km SOUTH OF ALASKA
2008 05 29 15:46:00  64.004N  21.012W M6.2  10.0km ICELAND
2008 06 08 12:25:29  37.963N  21.525W M6.3  16.0km SOUTHERN GREECE
2008 07 05 02:12:04  53.882N 152.886E M7.7 632.8km SEA OF OKHOTSK
2008 07 08 09:13:07  15.986S  71.748W M6.2 123.0km SOUTHERN PERU
2008 07 15 03:26:34  35.800S  27.860W M6.4  52.0km DODECANESE ISLANDS
2008 08 11 23:38:38   1.020N  21.843W M6.0  13.0km CENTRAL MID ATLANTIC RIDGE
2008 08 26 21:00:36   7.641S  74.377W M6.4 154.0km PERU BRAZIL BORDER REGION
2008 08 28 15:22:23   0.248S  17.357W M6.3  15.0km NORTH OF ASCENSION ISLAND
2008 09 03 11:25:13  26.569S  63.181W M6.0 547.4km SANTIAGO DEL ESTERO PROV., ARG
2008 09 10 13:08:14   8.092N  38.718W M6.6  10.0km CENTRAL MID ATLANTIC RIDGE
2008 09 24 02:33:05  17.607N 105.500W M6.4  10.0km OFF COAST OF JALISCO, MEXICO
2008 10 11 10:40:14  19.161N  64.833W M6.1  23.0km VIRGIN ISLANDS
2008 10 12 20:55:41  20.123S  64.971W M6.2 352.7km SOUTHERN BOLIVIA
2008 10 16 19:41:25  14.423N  92.364W M6.6  24.0km NEAR COAST OF CHIAPAS, MEXICO
```

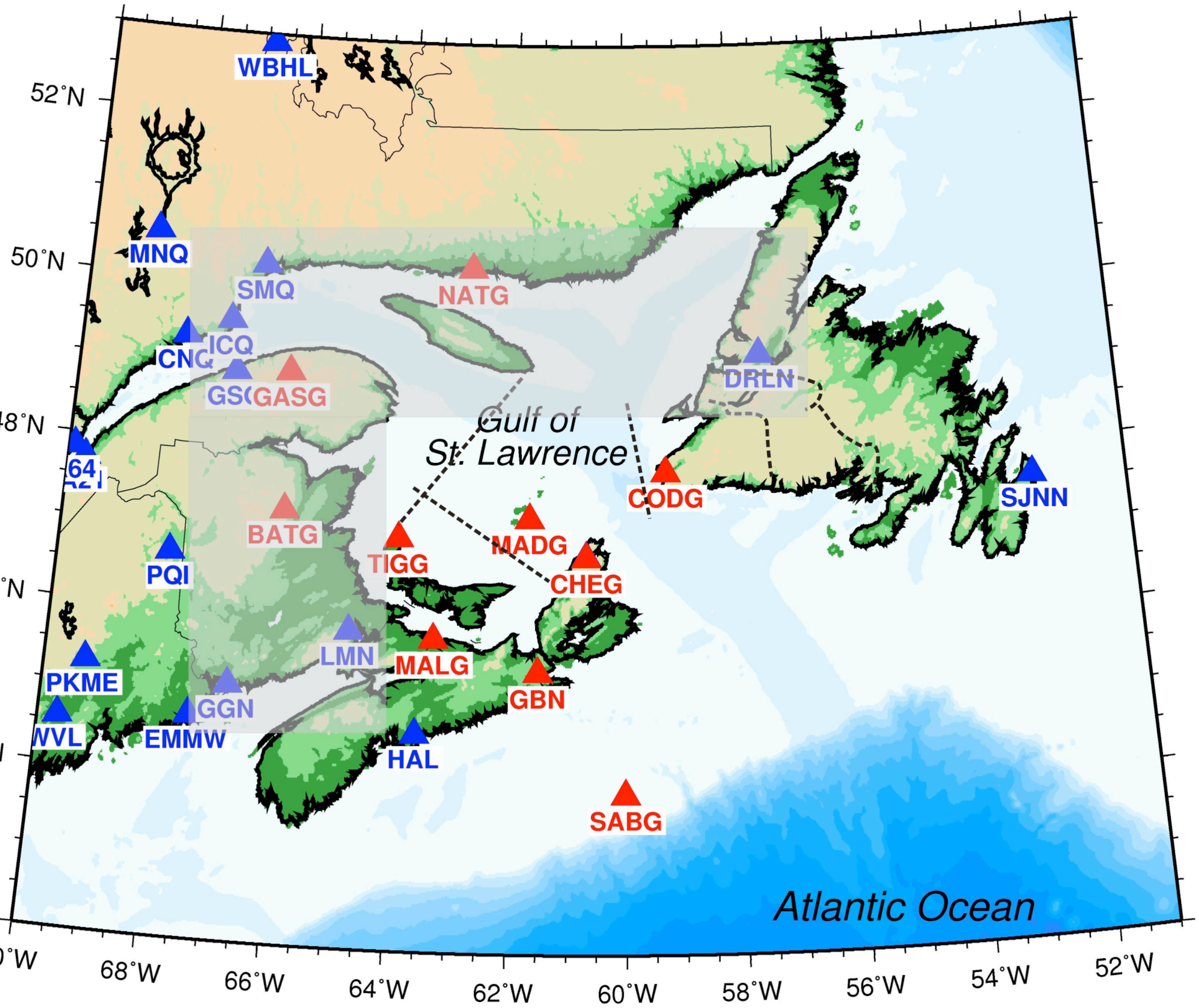

Figure 1. Map showing the station distribution of the Atlantic array (red triangles). Geographic coordinates of each station are listed in Table 1. Permanent stations of the Canadian National Seismograph Network (CNSN) are marked by blue triangles. Approximate locations of the LITHOPROBE reflection and refraction profiles are marked by thick black dashed lines. Thin black lines marks provincial boundaries. The gray-shaded area corresponds to the two velocity profiles shown in Figure 34.

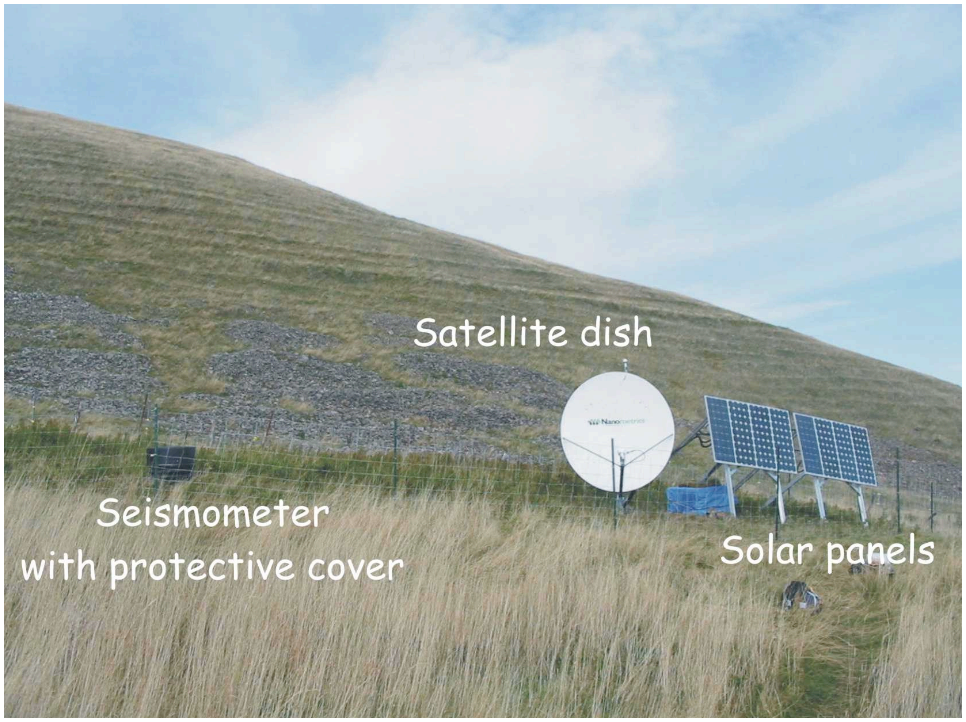

Figure 2. Station MADG on the Magdalen Islands, showing the solar panels, satellite dish, and the protective vault over the seismometer.

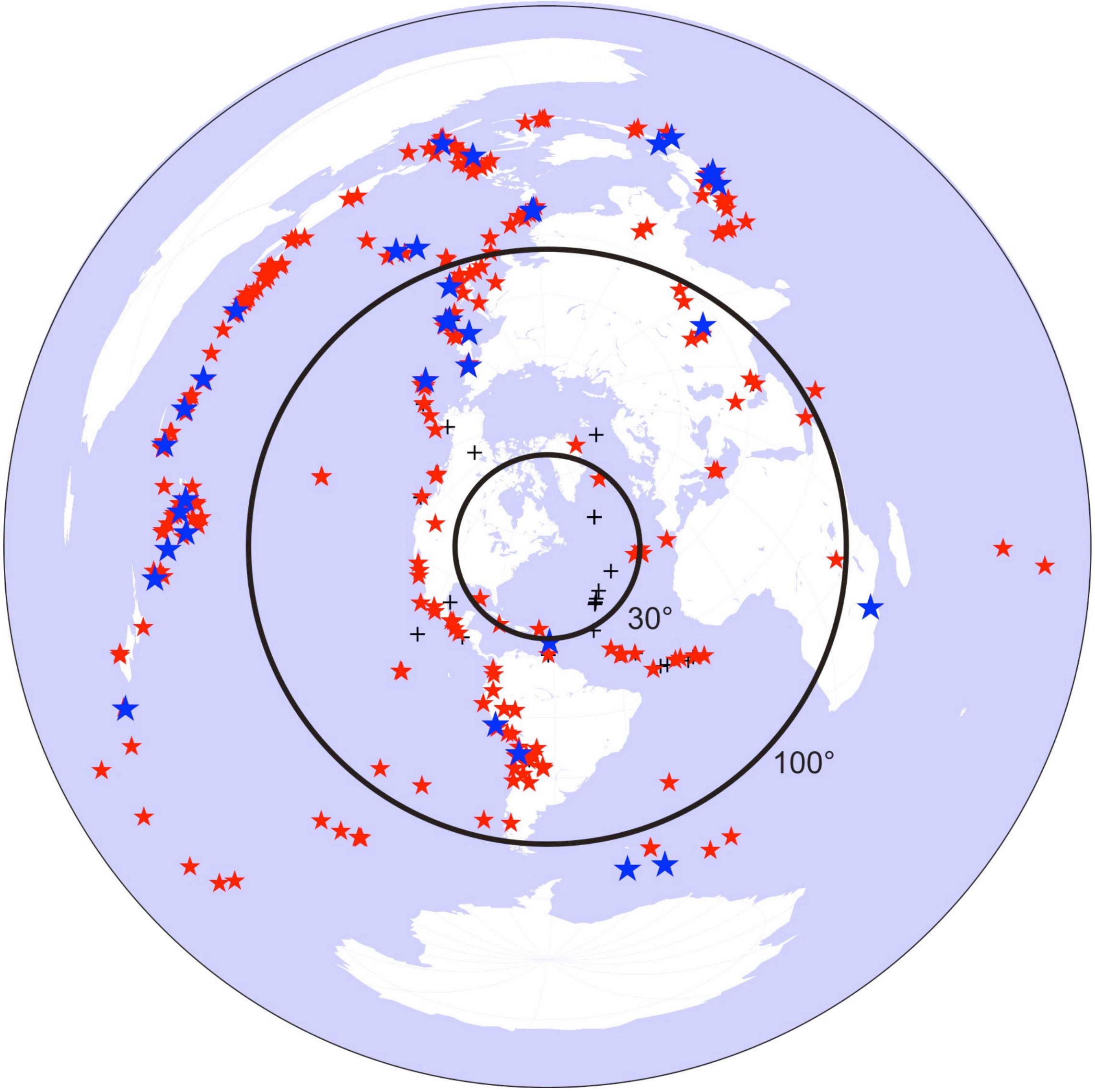

Figure 3. Map showing epicenters of large earthquakes listed in Table 2. Large blue stars are events with M 7.0 or larger; medium red stars are M between 6.0 and 6.9; and small black crosses are M between 5.0 and 5.9. Solid circles outline distance ranges suitable for receiver function analysis used in this study.

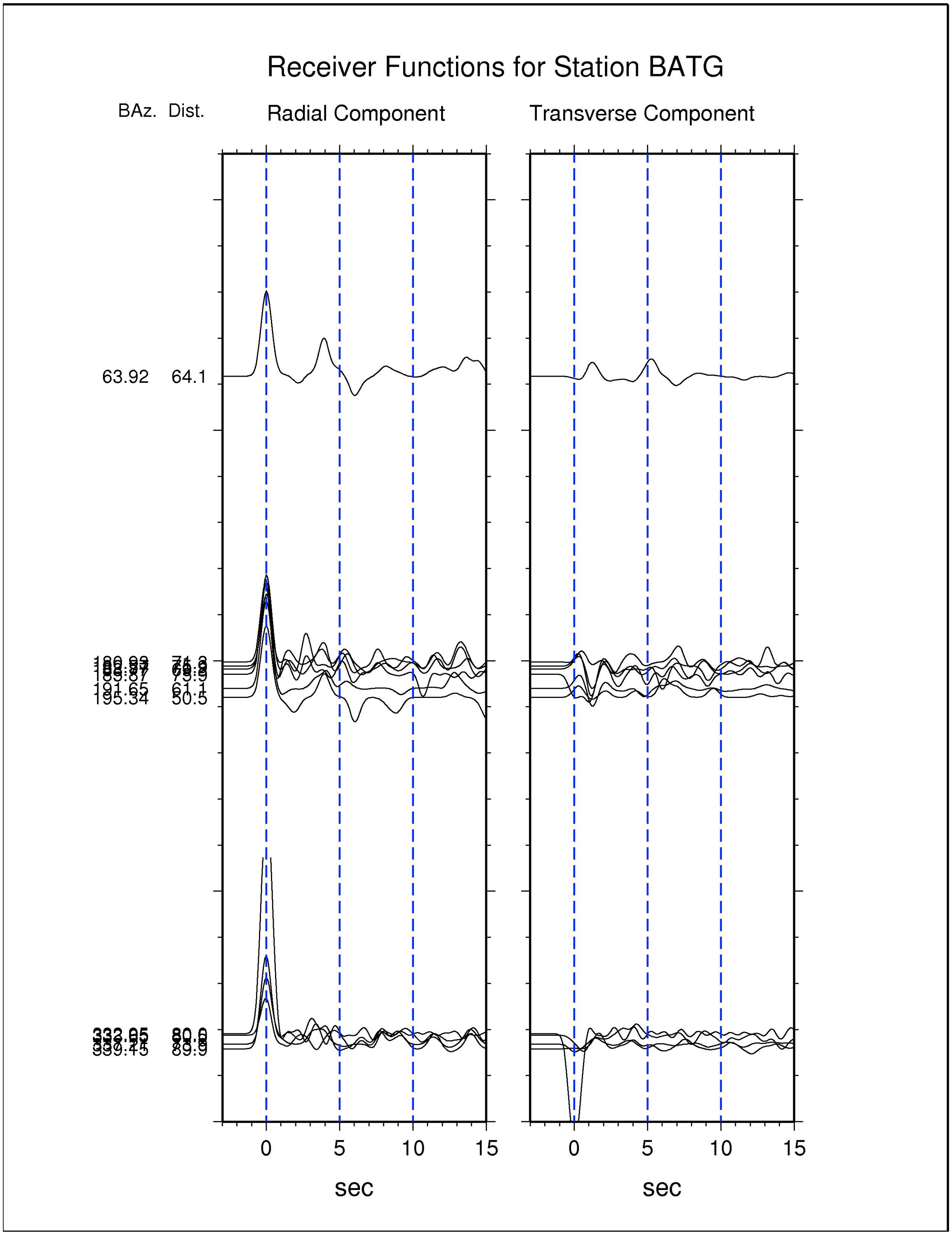

Figure 4. Receiver functions of the station BATG. Traces are arranged according to the source event's back azimuth, shown as the first number to the left side of each receiver function pair. The second number corresponds to the event's distance. The water-filling parameter (A) is set to 2, corresponding to the long-period frequency band.

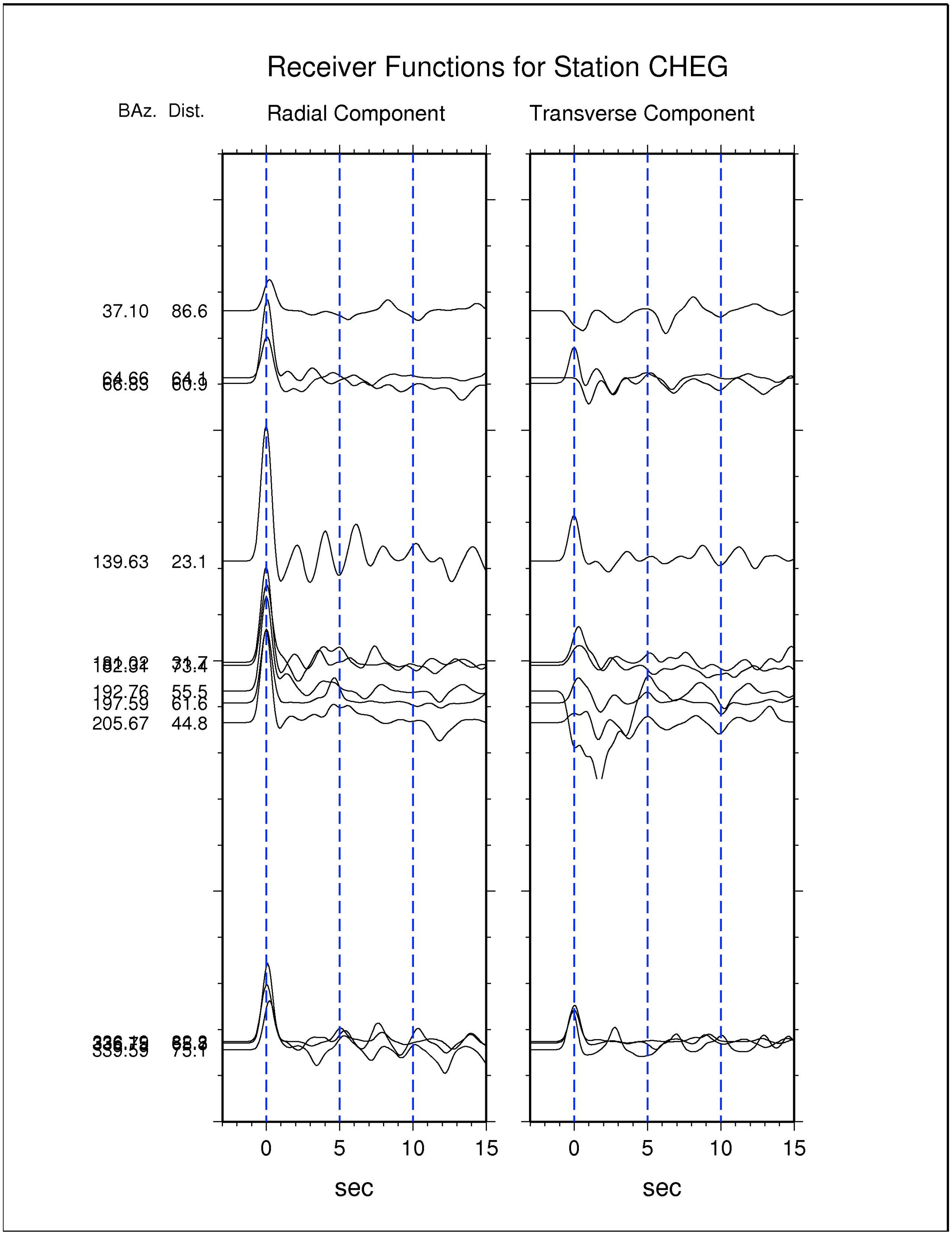

Figure 5. Long-period receiver functions of the station CHEG. Layout is the same as that in Figure 4.

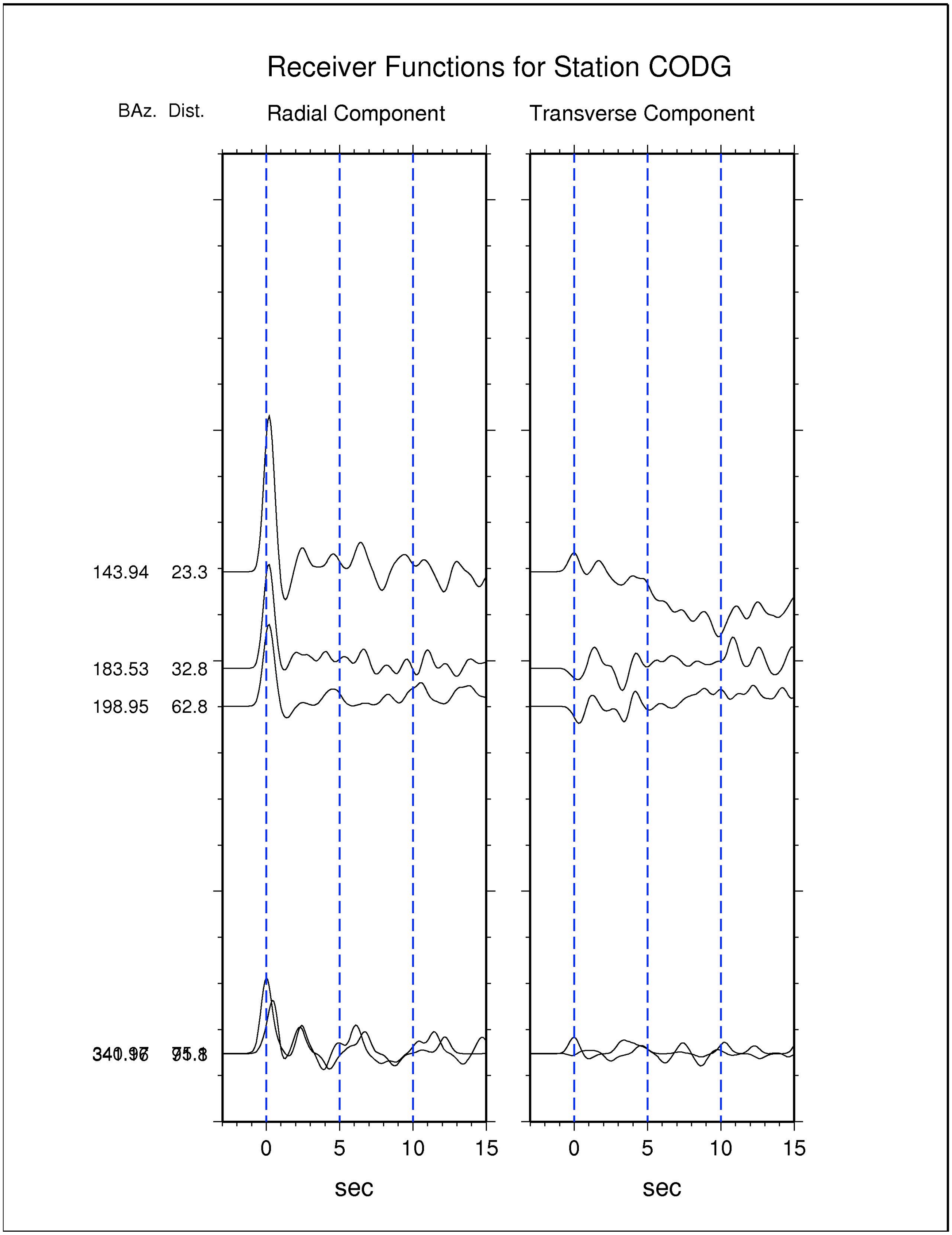

Figure 6. Long-period receiver functions of the station CODG. Layout is the same as that in Figure 4.

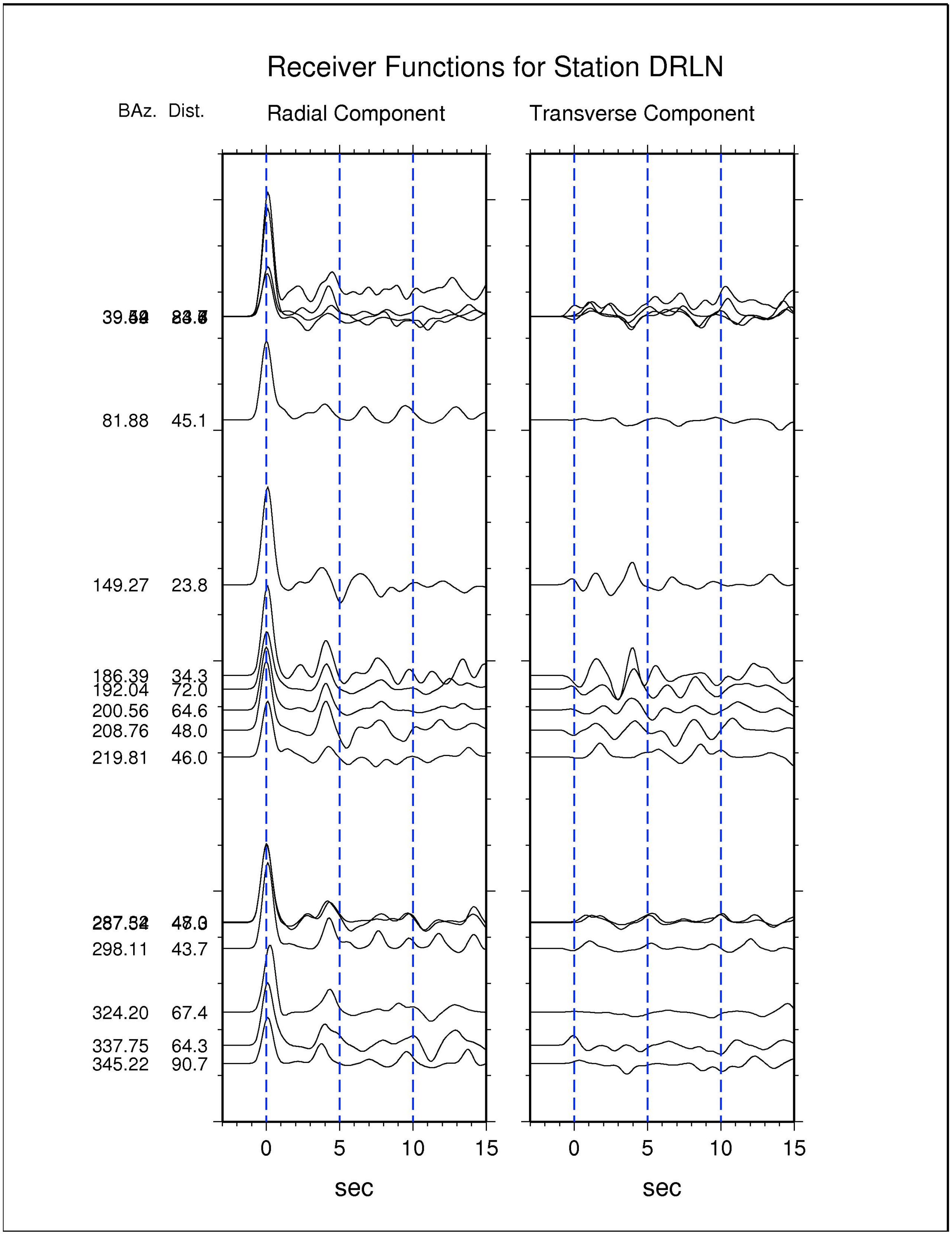

Figure 7. Long-period receiver functions of the station DRLN. Layout is the same as that in Figure 4.

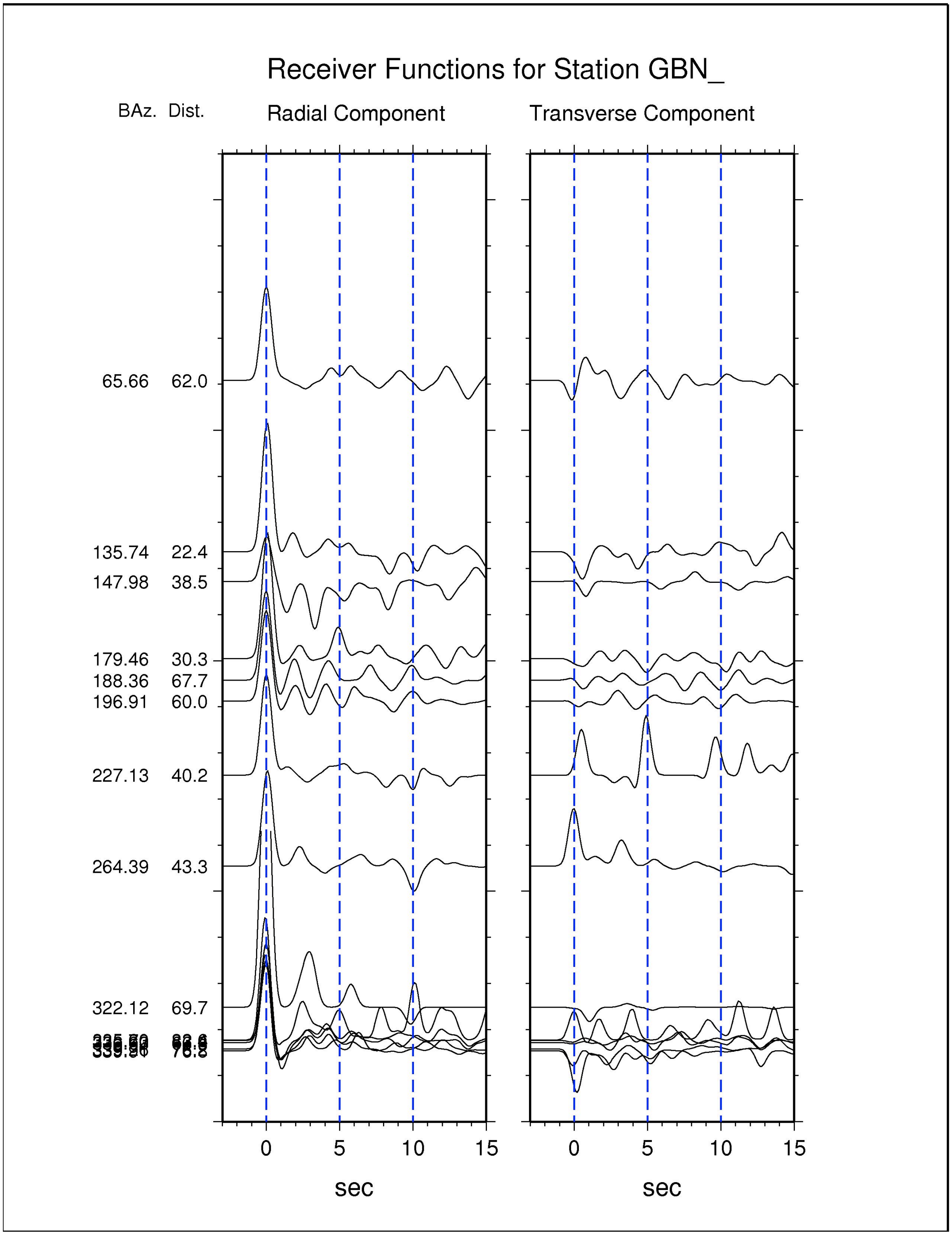

Figure 8. Long-period receiver functions of the station GBN. Layout is the same as that in Figure 4.

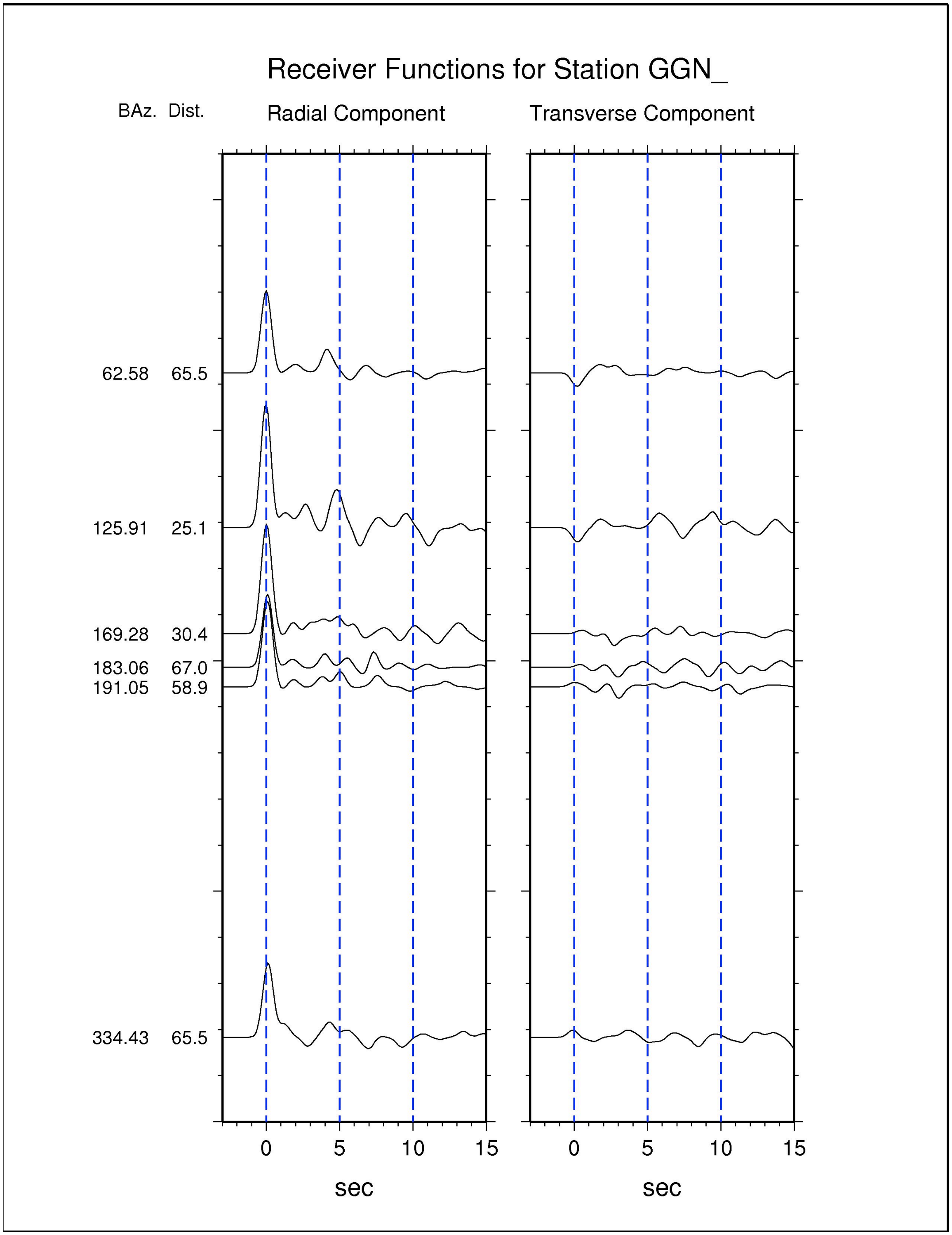

Figure 9. Long-period receiver functions of the station GGN. Layout is the same as that in Figure 4.

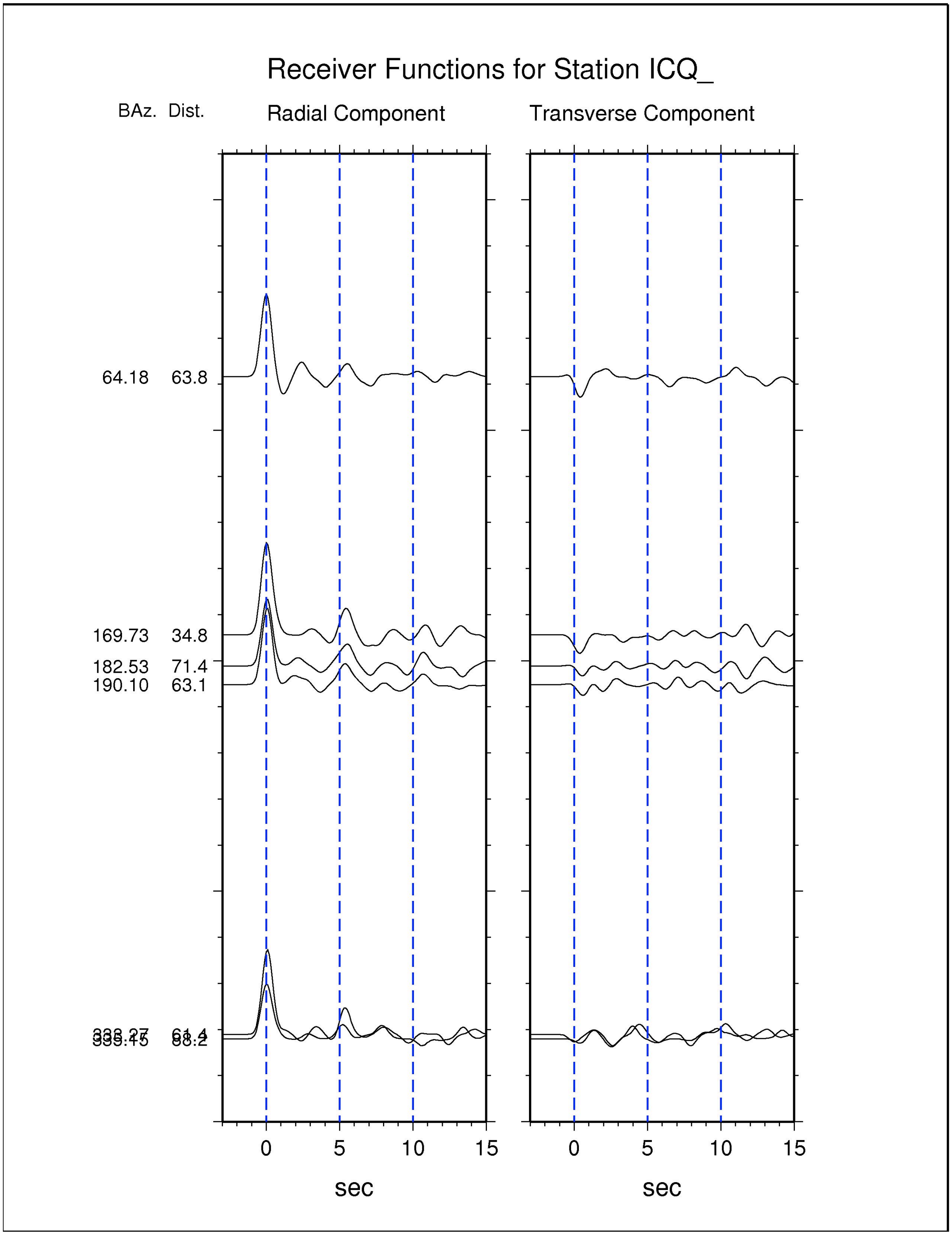

Figure 10. Long-period receiver functions of the station ICQ. Layout is the same as that in Figure 4.

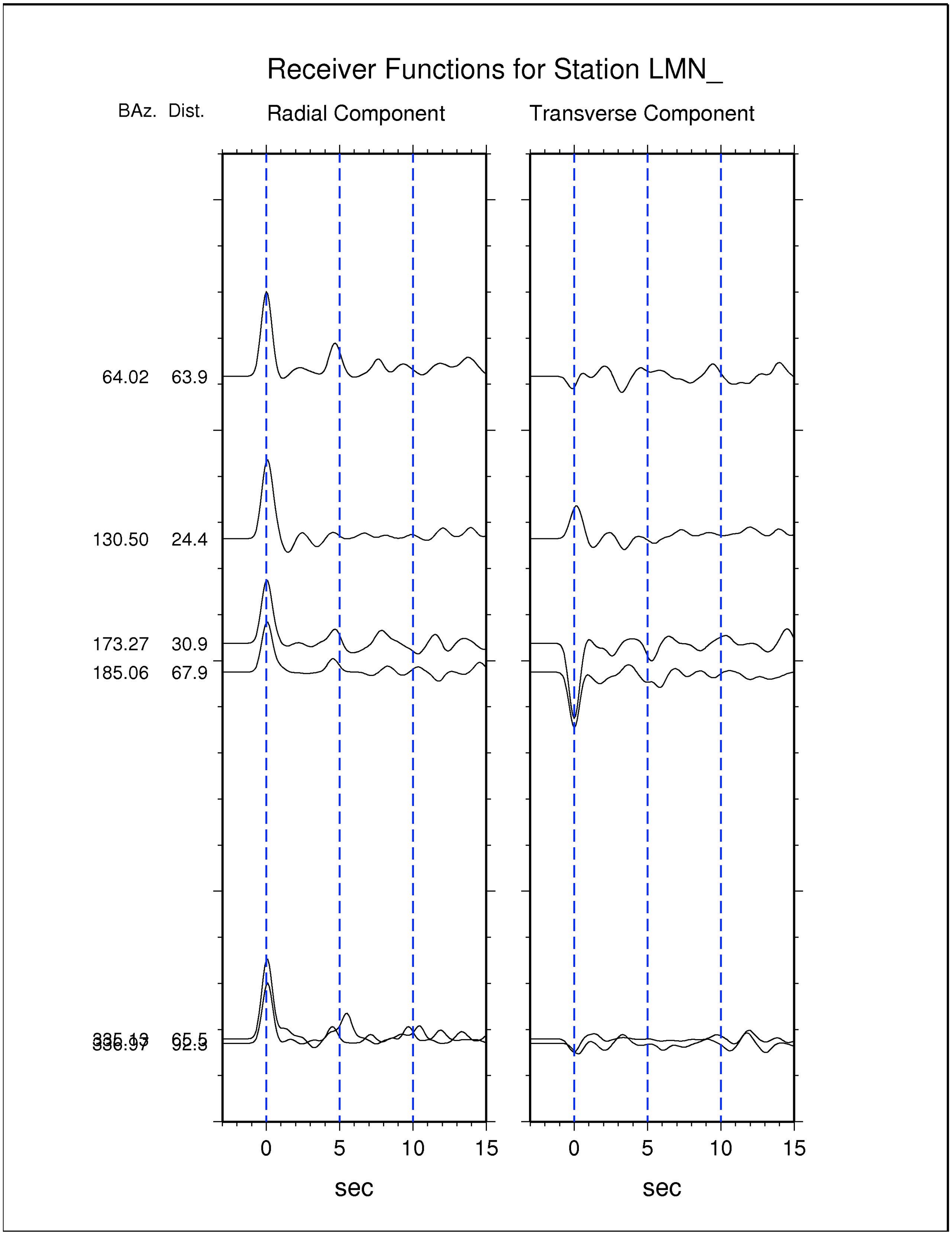

Figure 11. Long-period receiver functions of the station LMN. Layout is the same as that in Figure 4.

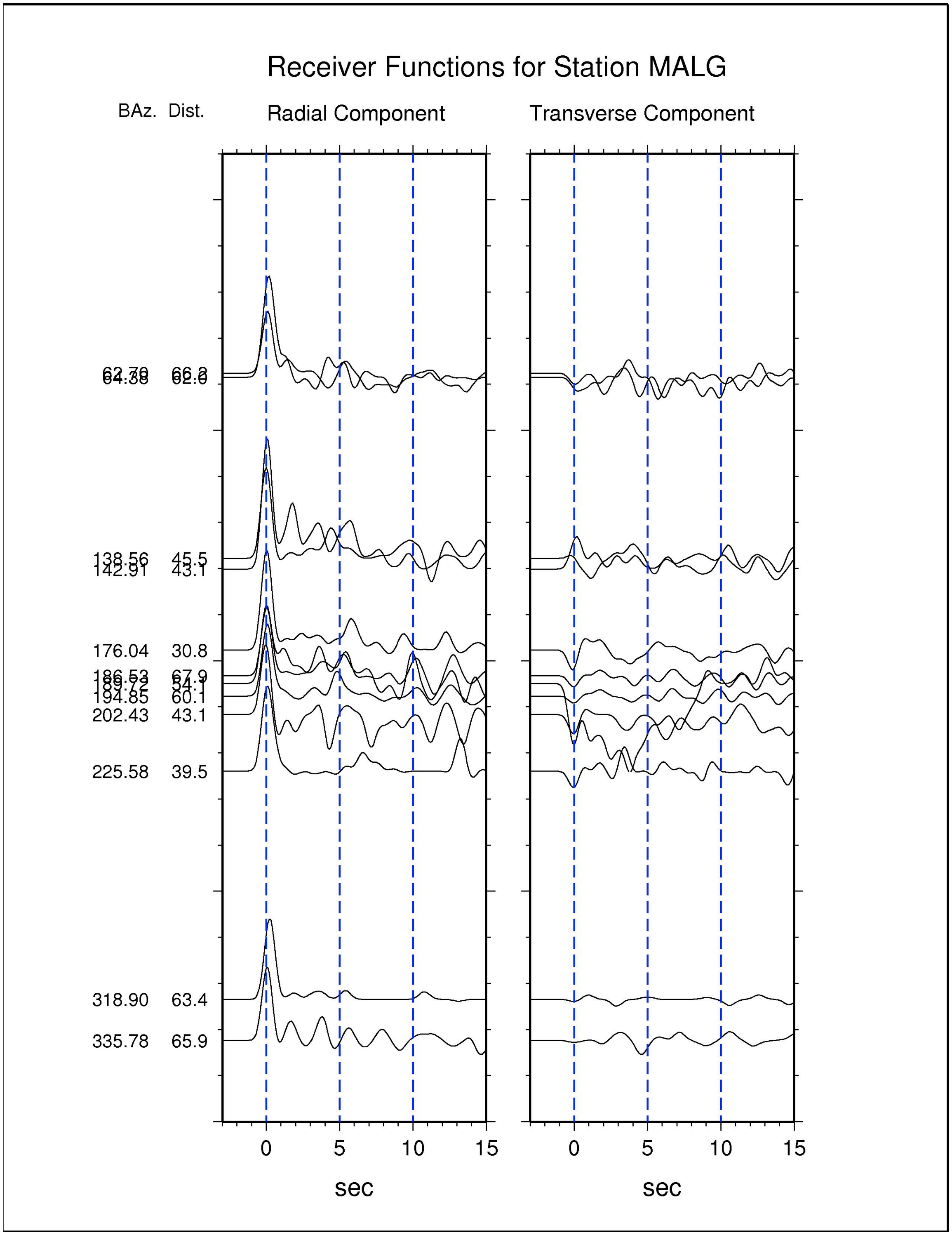

Figure 12. Long-period receiver functions of the station MALG. Layout is the same as that in Figure 4.

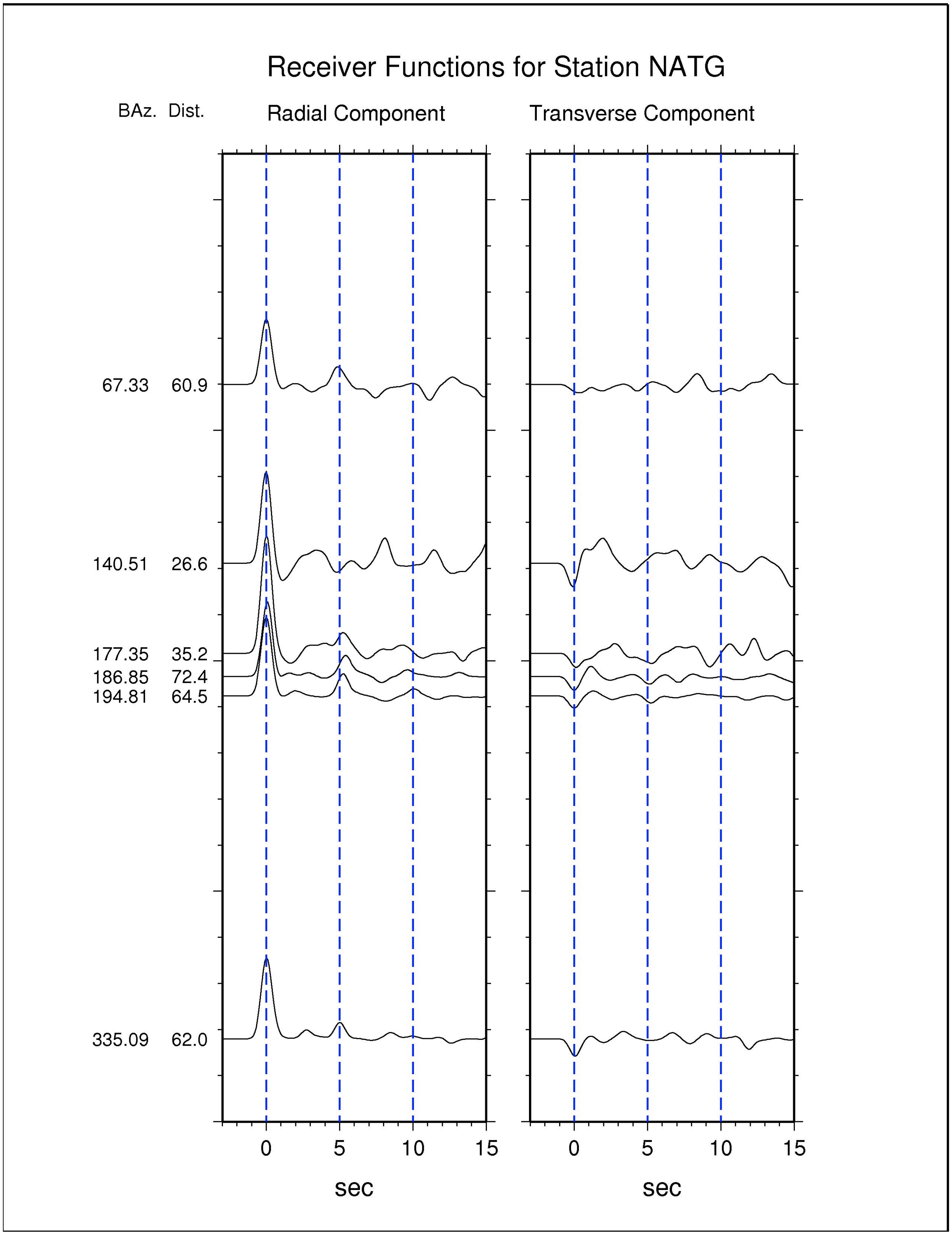

Figure 13. Long-period receiver functions of the station NATG. Layout is the same as that in Figure 4.

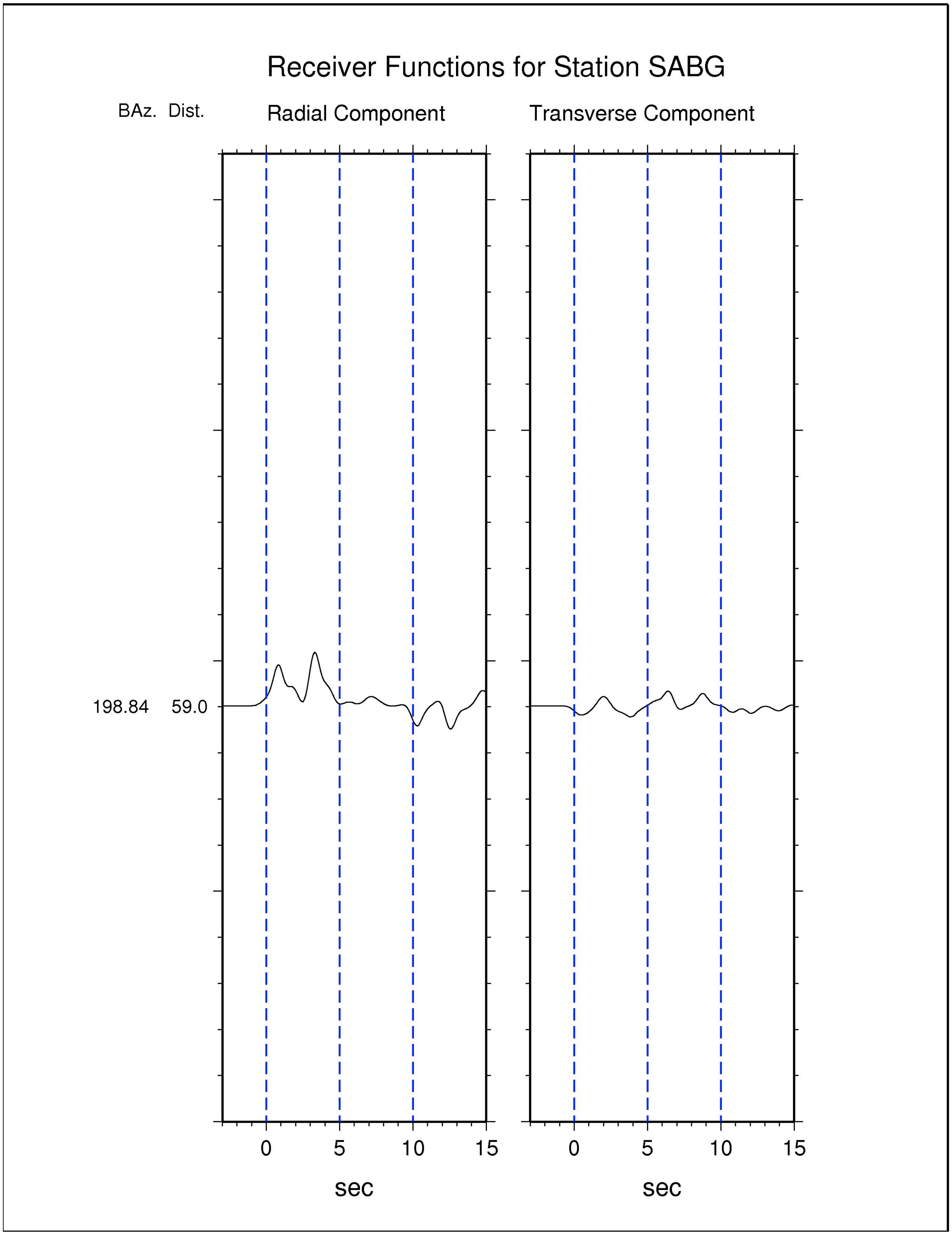

Figure 14. Long-period receiver functions of the station SABG. Layout is the same as that in Figure 4.

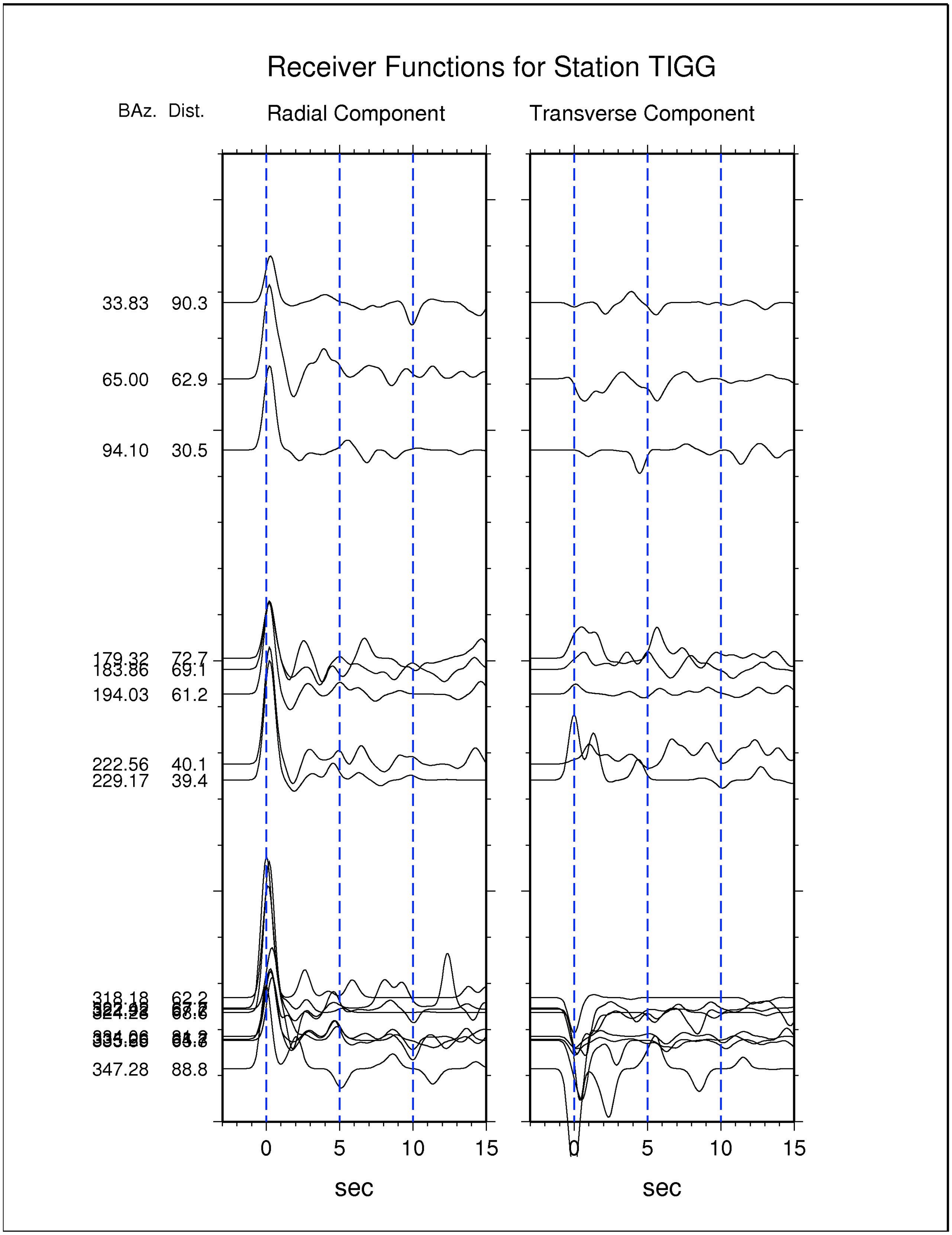

Figure 15. Long-period receiver functions of the station TIGG. Layout is the same as that in Figure 4.

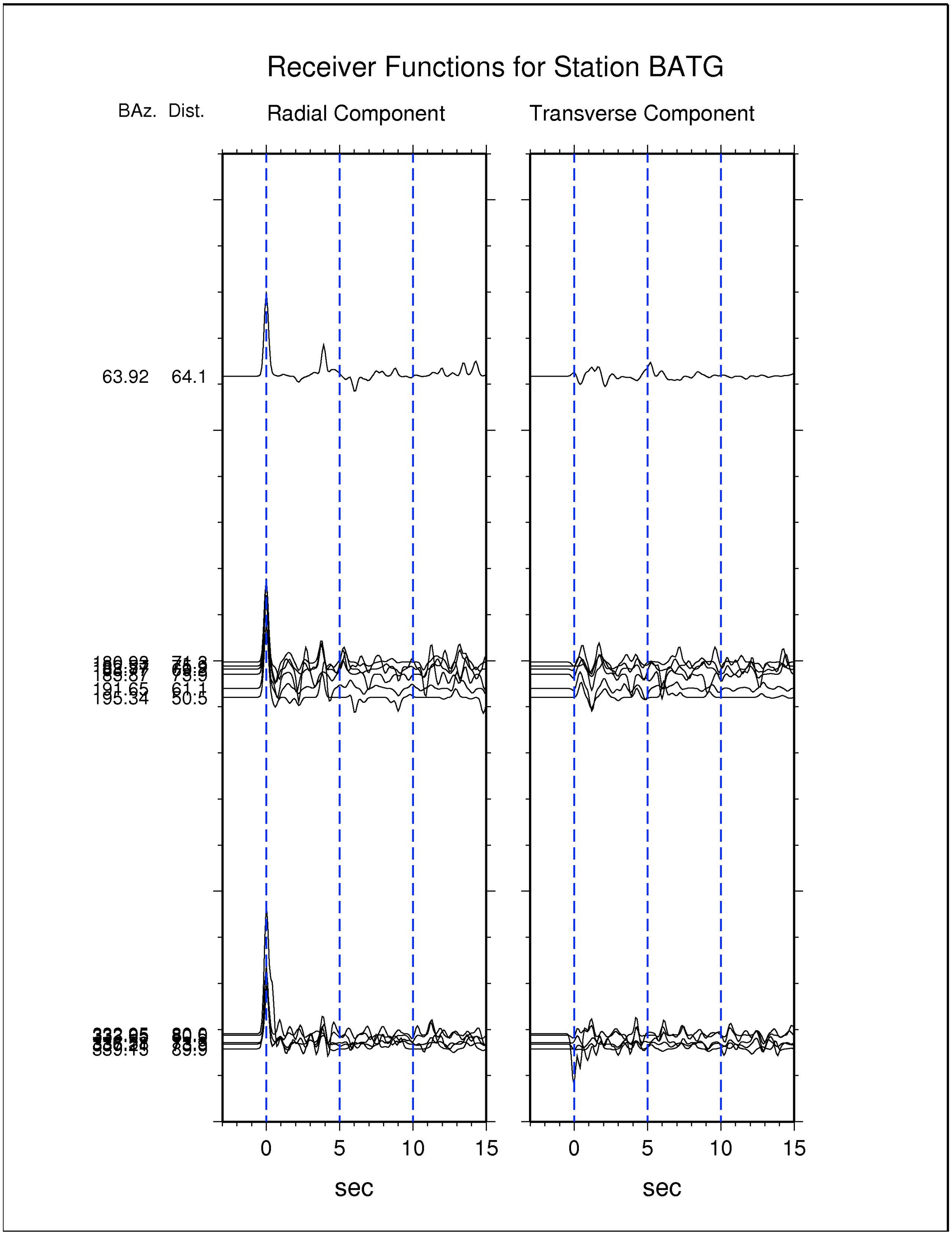

Figure 16. Receiver functions of the station BATG. The water-filling parameter (A) is set to 5, corresponding to the short-period frequency band. Layout is the same as that in Figure 4.

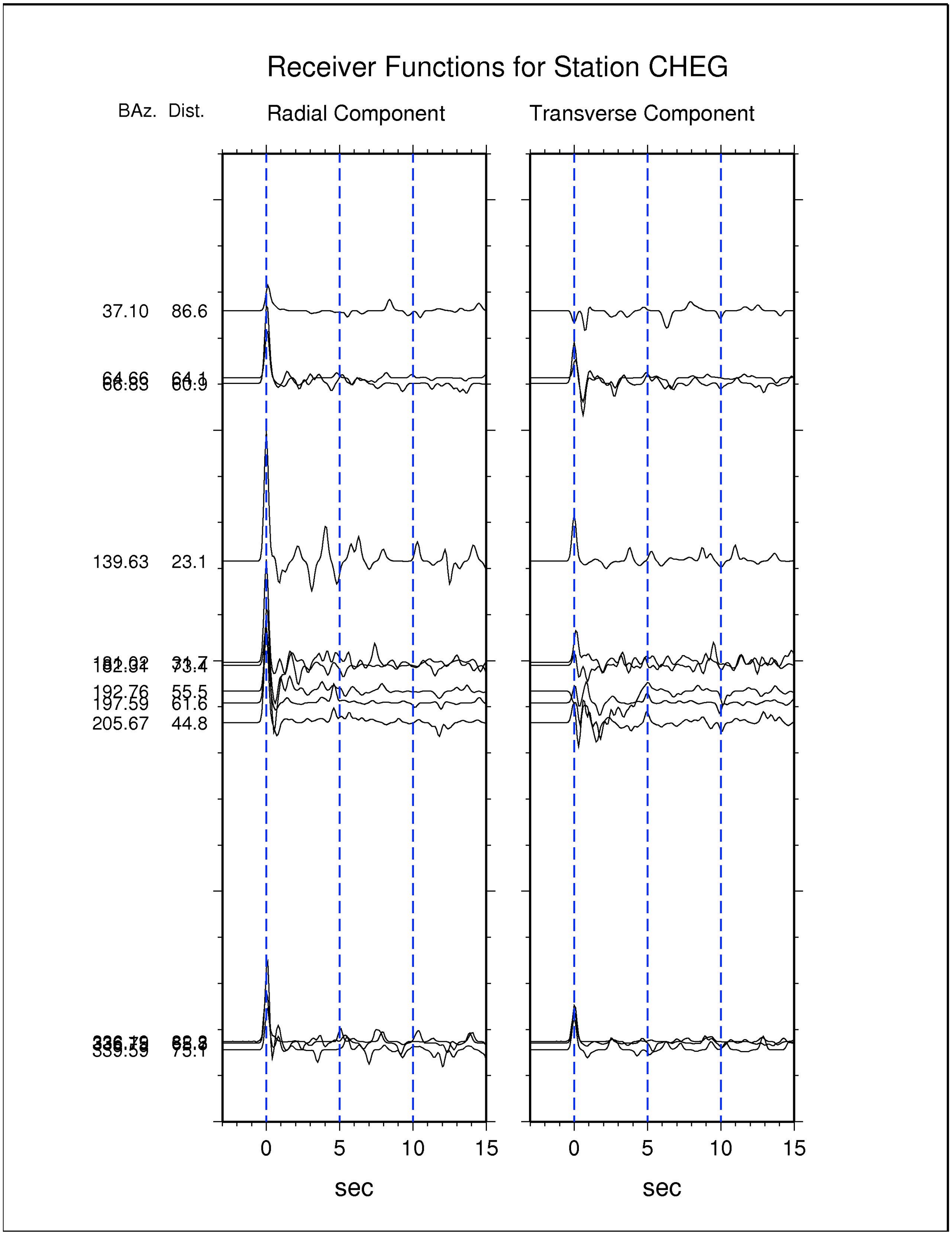

Figure 17. Short-period receiver functions of the station CHEG. Layout is the same as that in Figure 4.

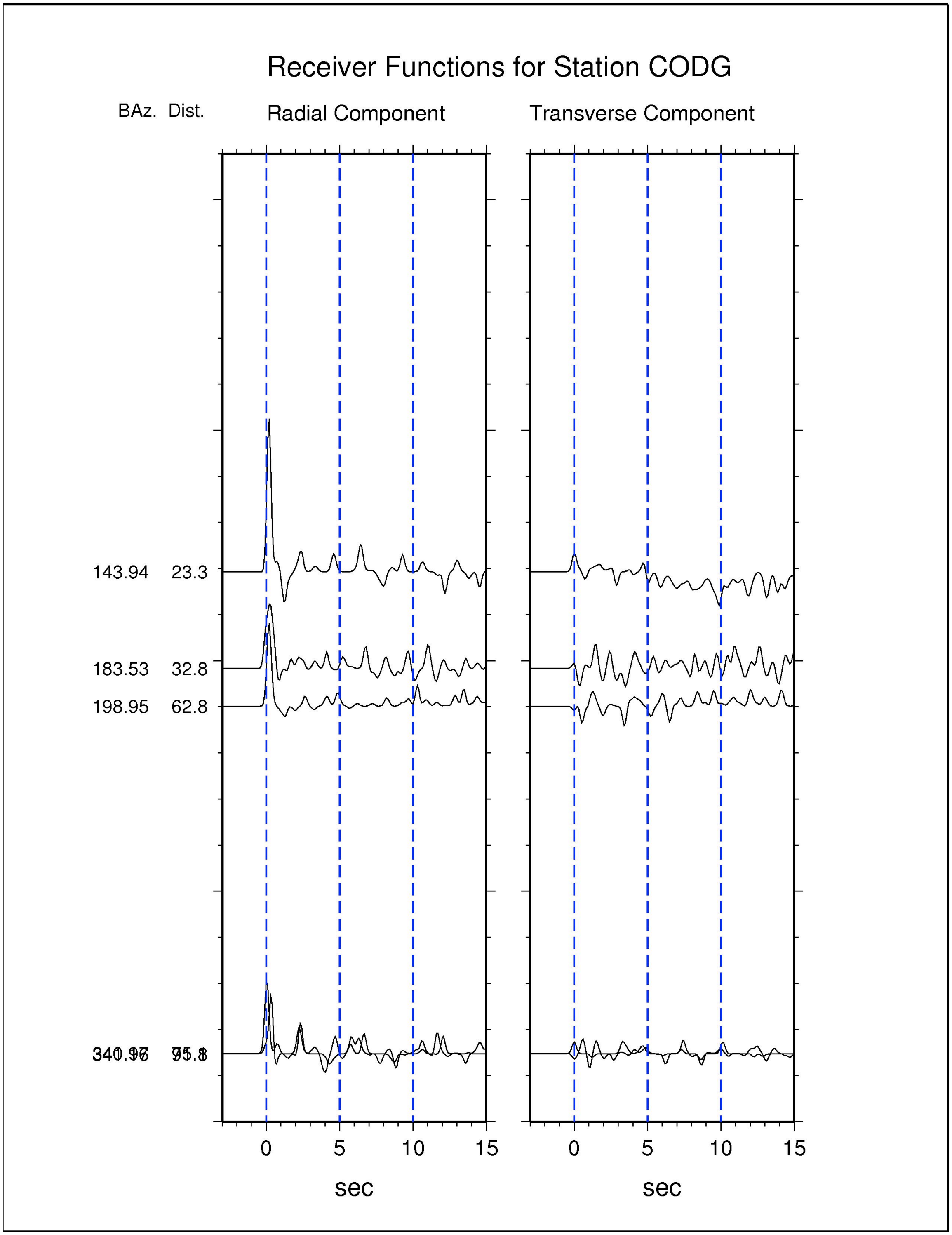

Figure 18. Short-period receiver functions of the station CODG. Layout is the same as that in Figure 4.

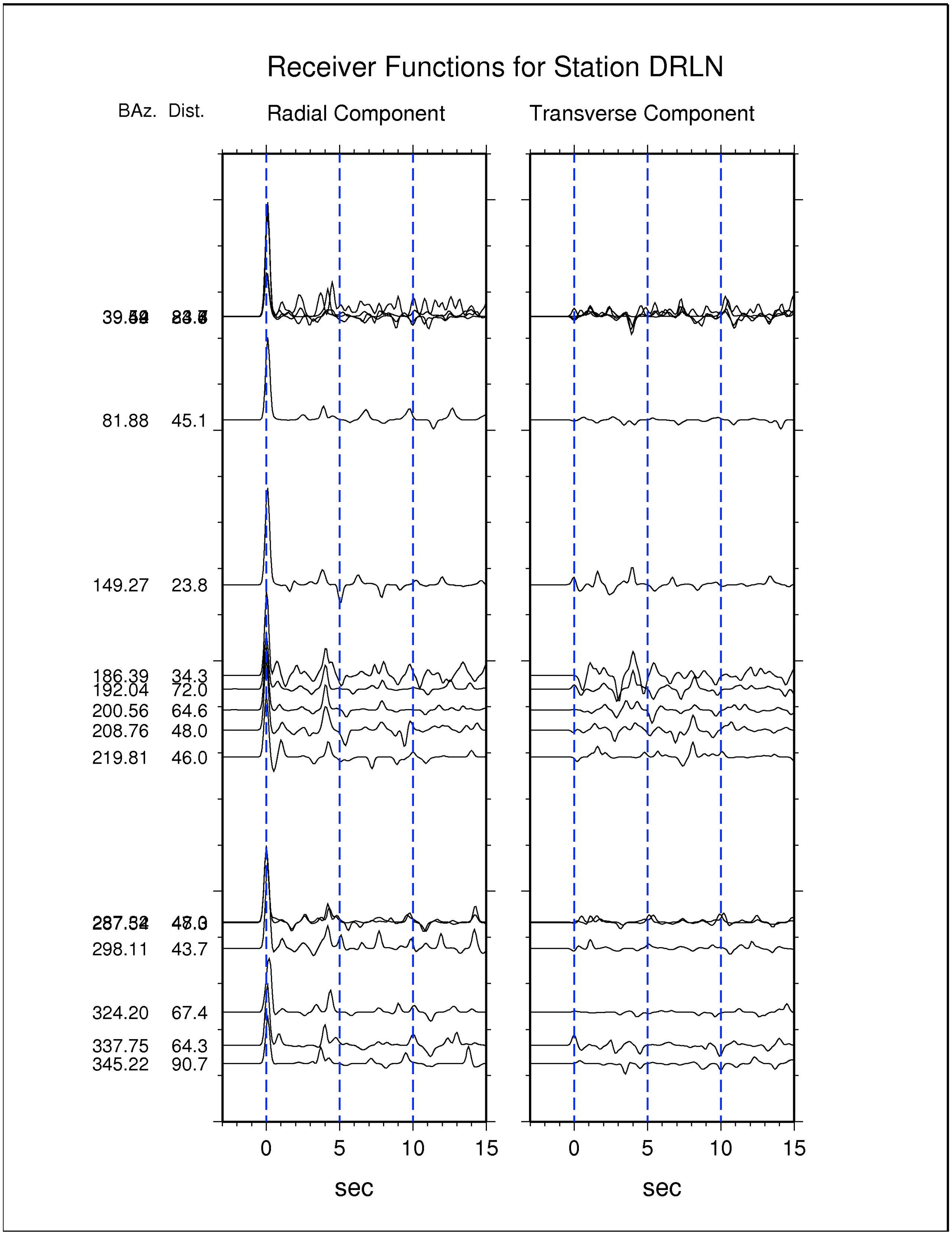

Figure 19. Short-period receiver functions of the station DRLN. Layout is the same as that in Figure 4.

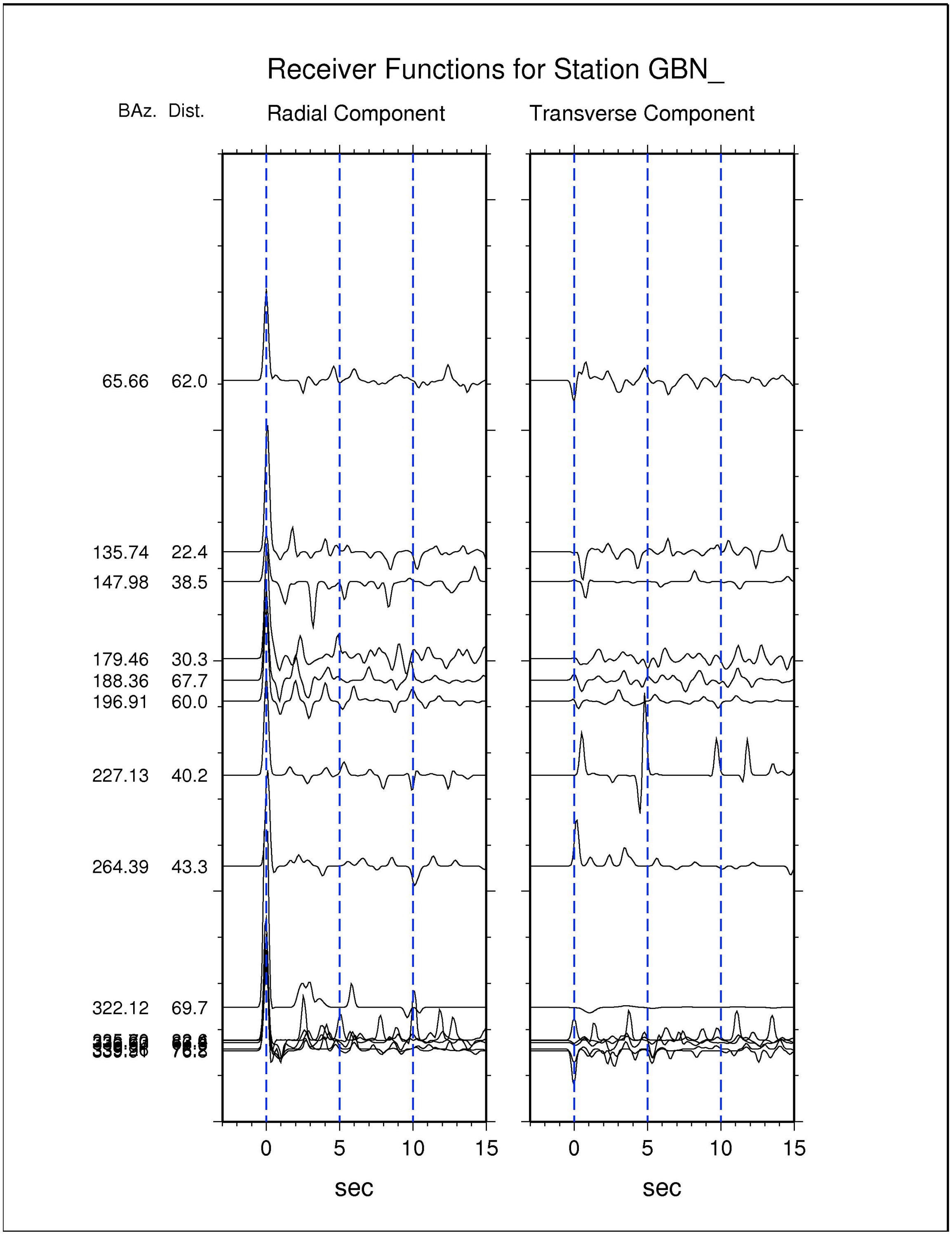

Figure 20. Short-period receiver functions of the station GBN. Layout is the same as that in Figure 4.

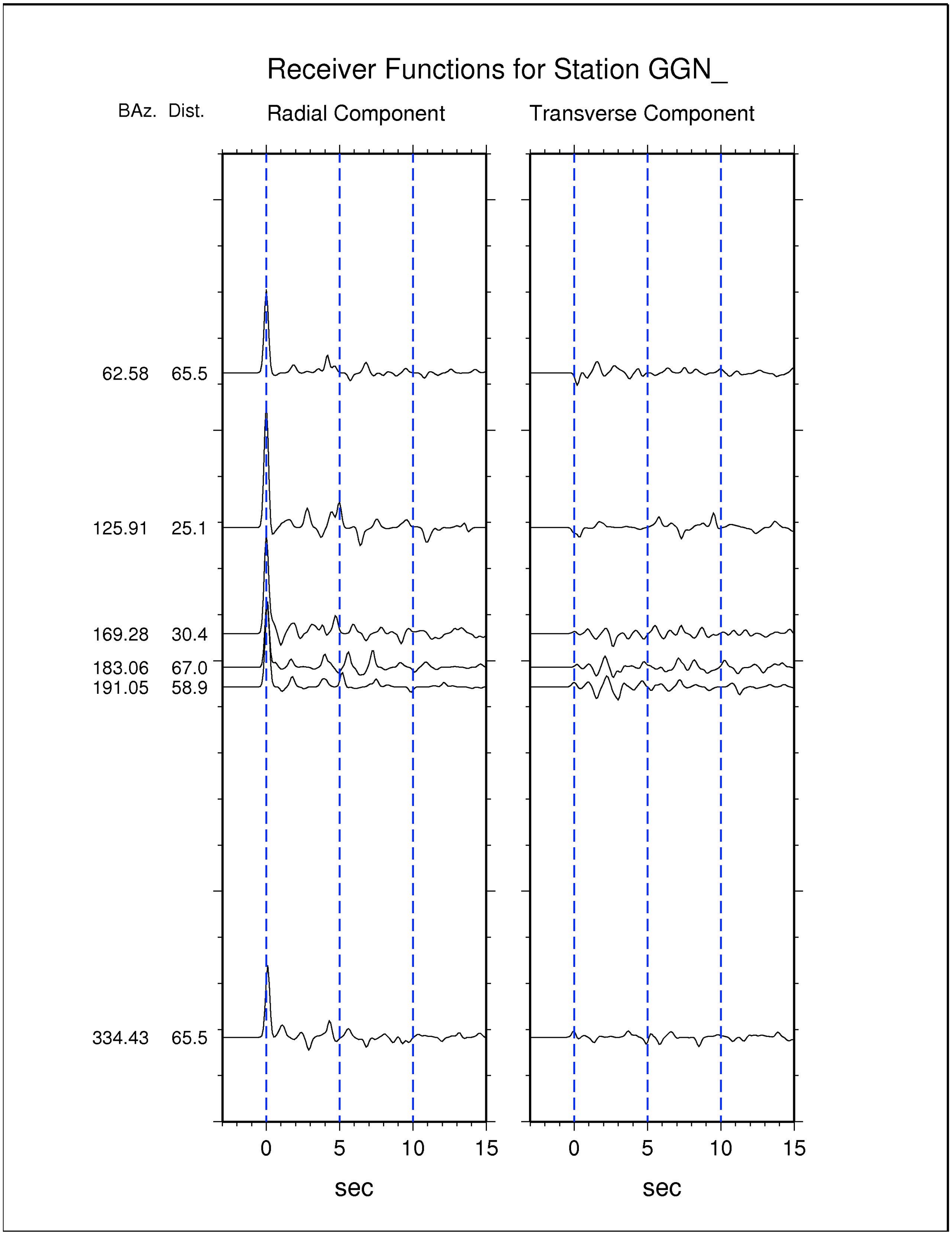

Figure 21. Short-period receiver functions of the station GGN. Layout is the same as that in Figure 4.

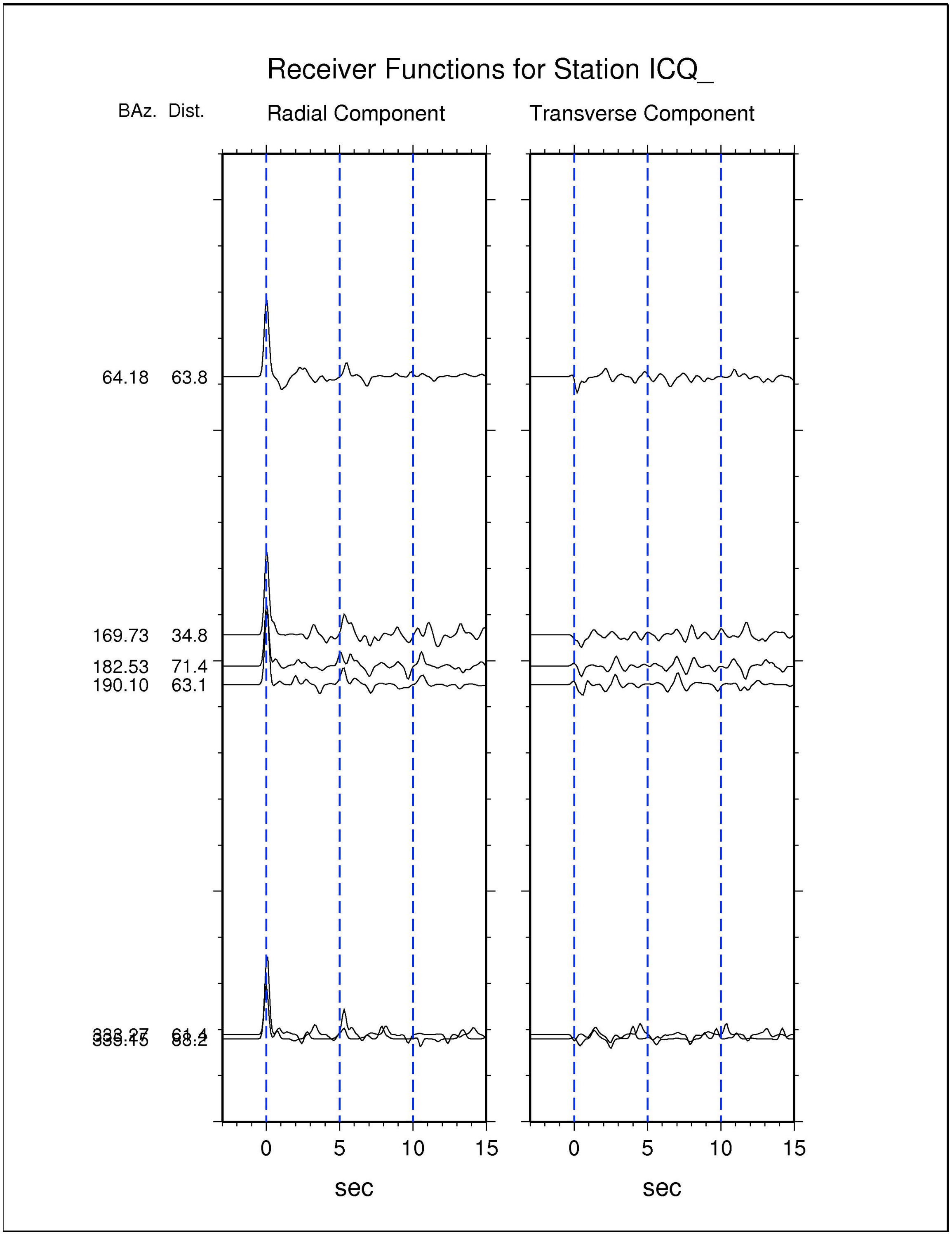

Figure 22. Short-period receiver functions of the station ICQ. Layout is the same as that in Figure 4.

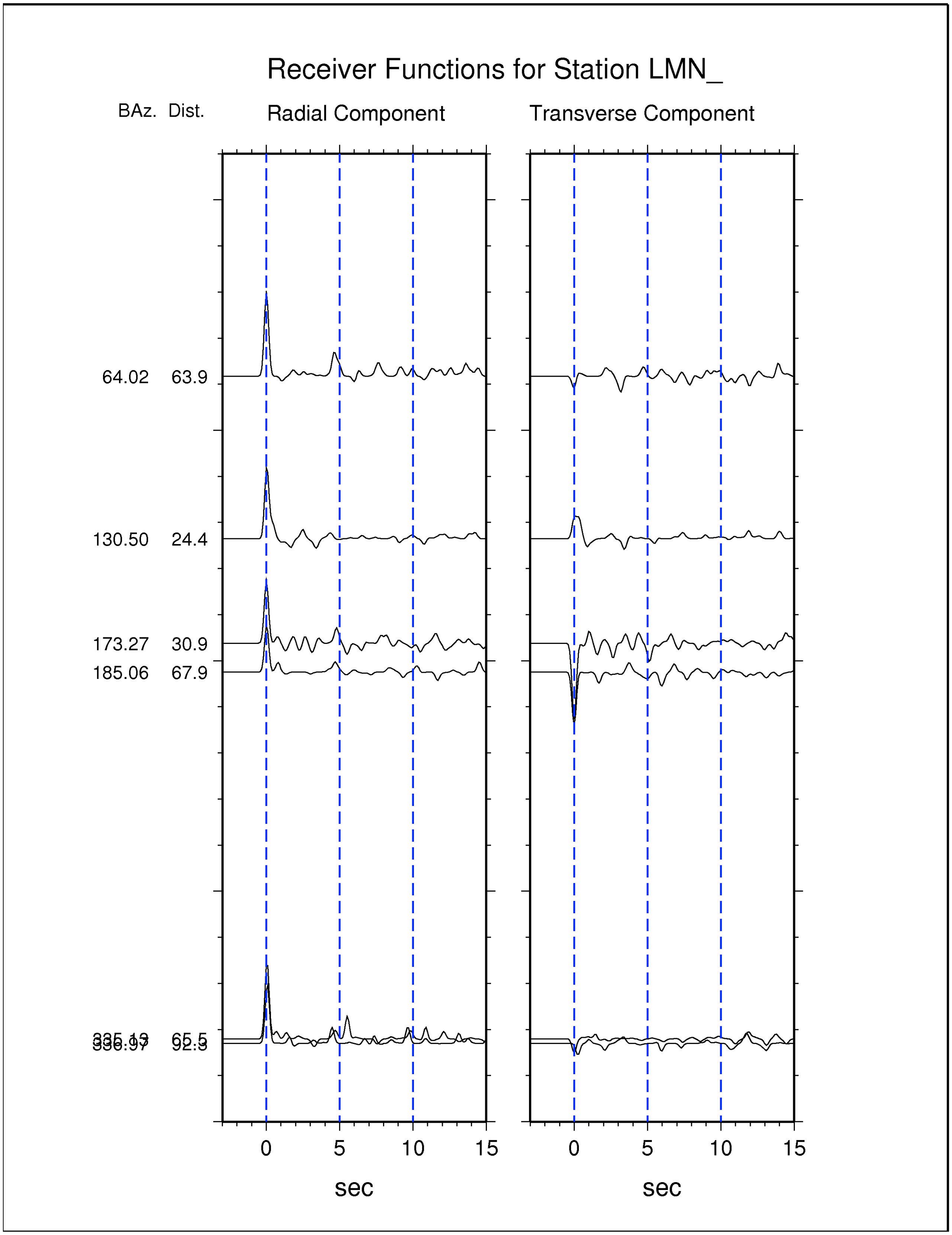

Figure 23. Short-period receiver functions of the station LMN. Layout is the same as that in Figure 4.

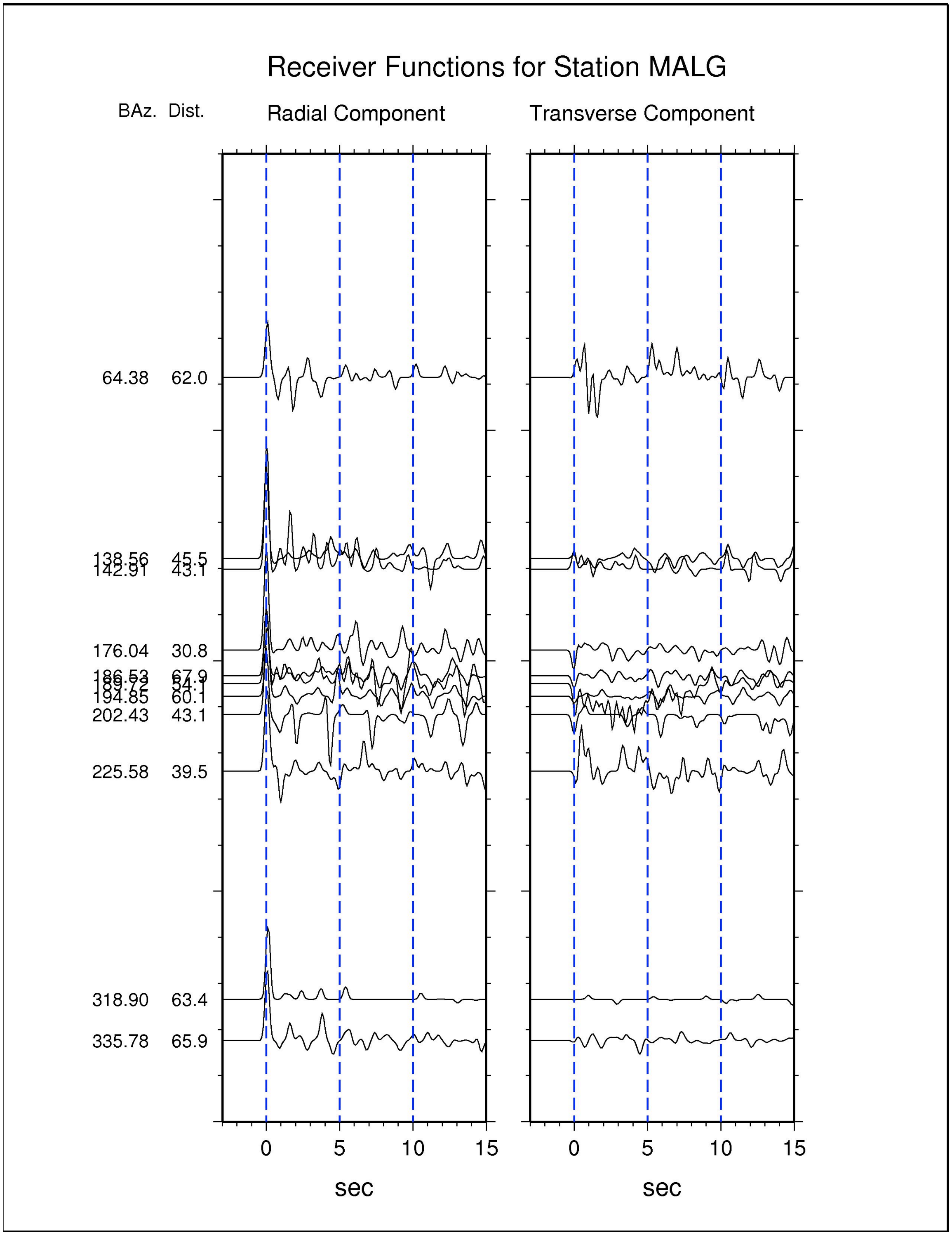

Figure 24. Short-period receiver functions of the station MALG. Layout is the same as that in Figure 4.

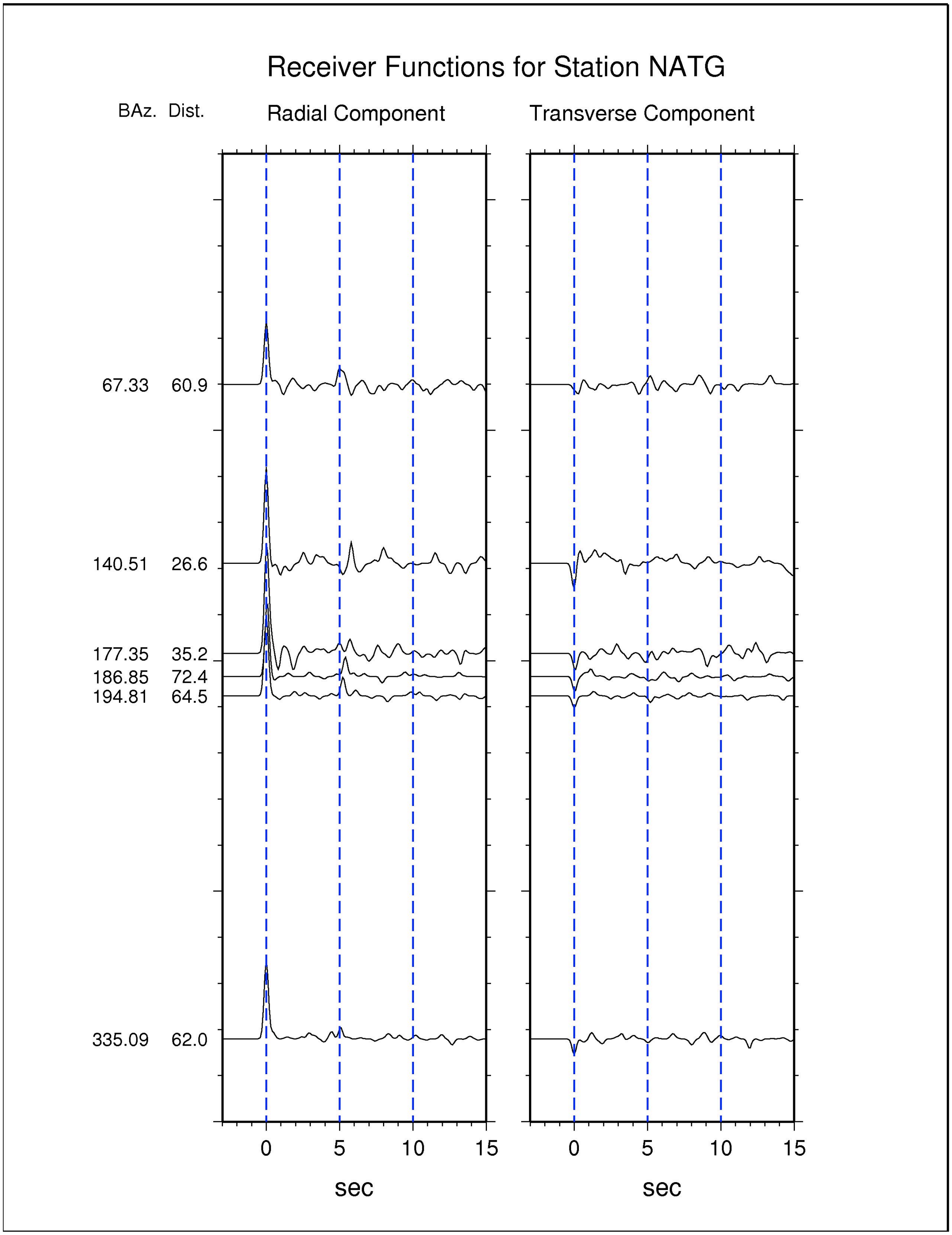

Figure 25. Short-period receiver functions of the station NATG. Layout is the same as that in Figure 4.

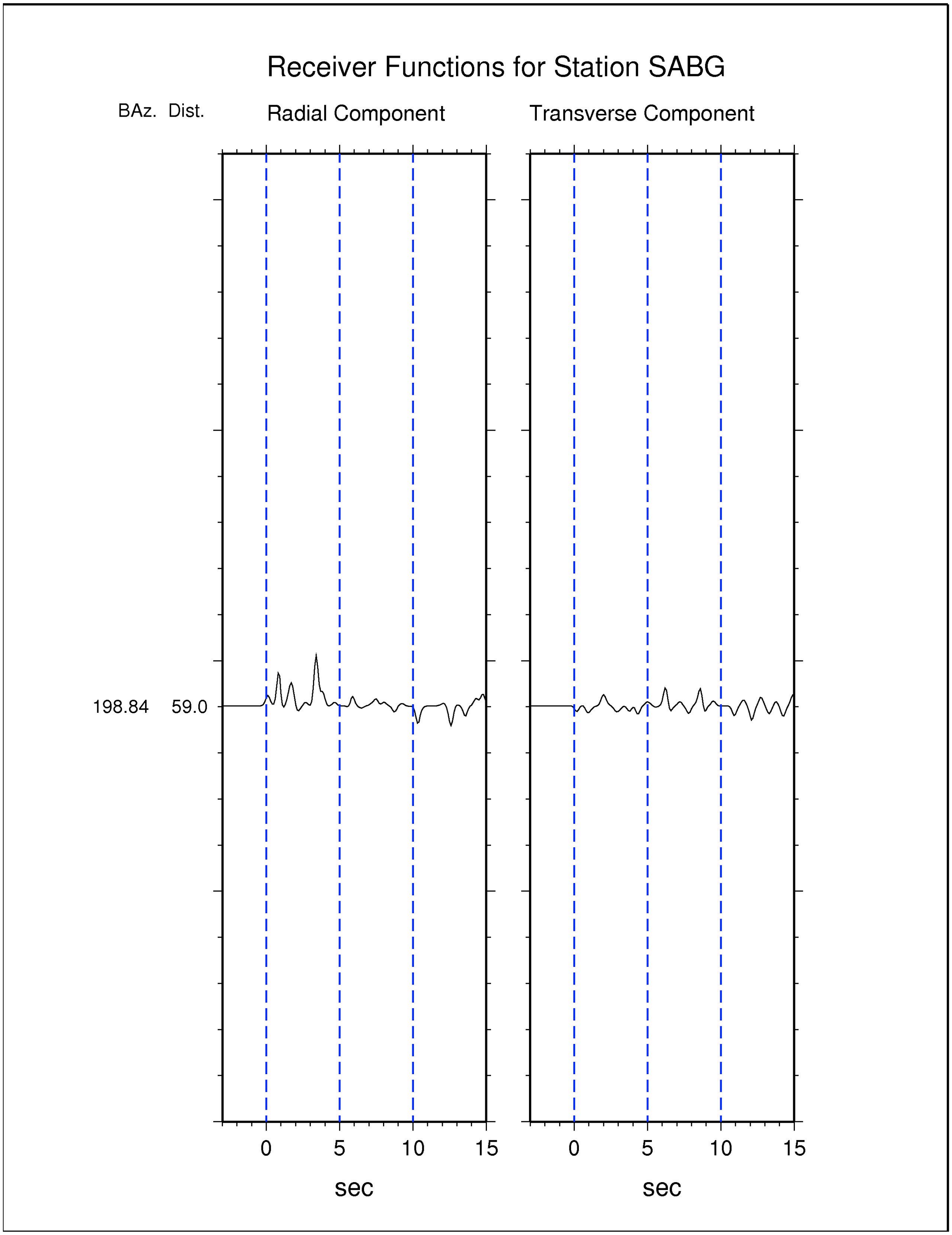

Figure 26. Short-period receiver functions of the station SABG. Layout is the same as that in Figure 4.

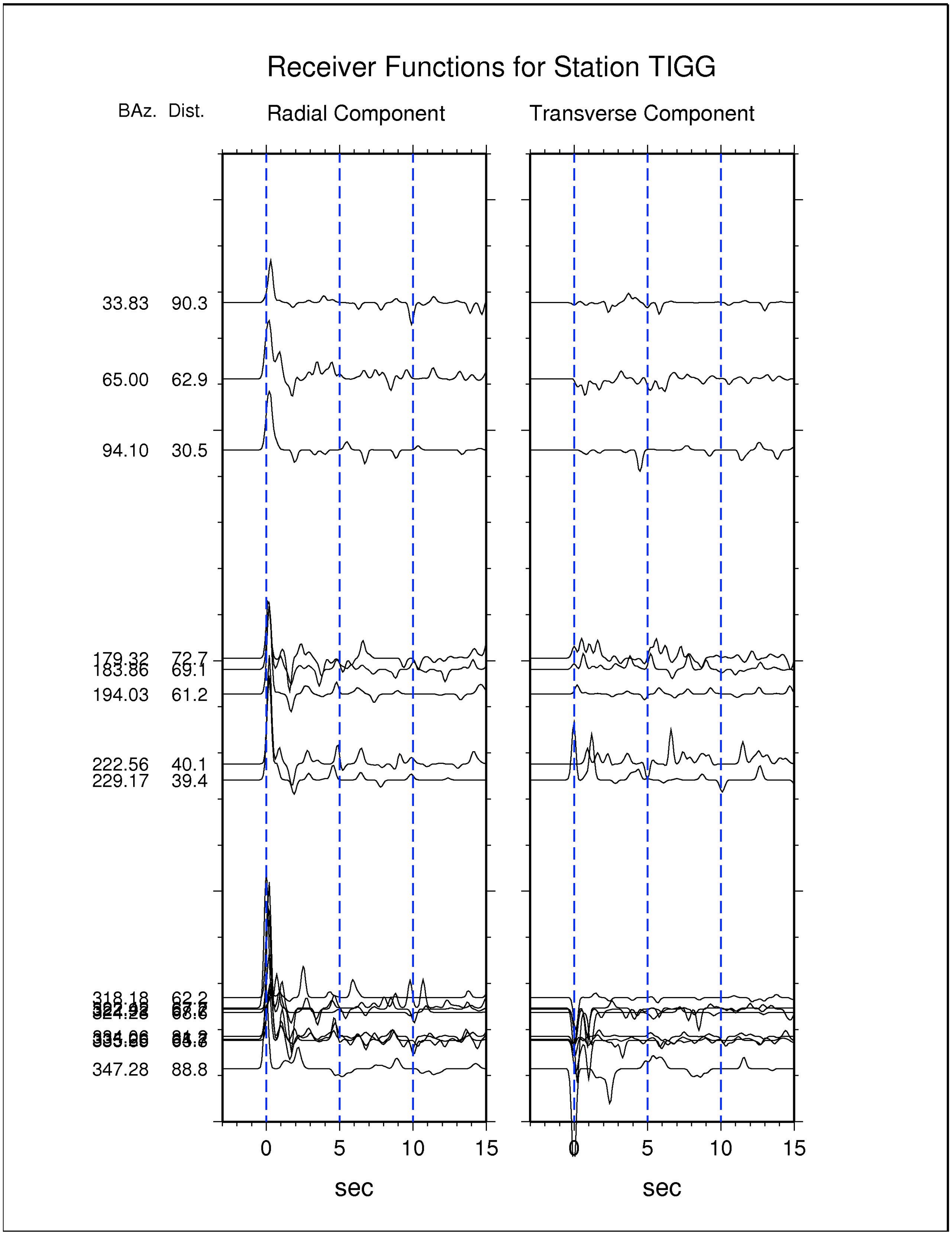

Figure 27. Short-period receiver functions of the station TIGG. Layout is the same as that in Figure 4.

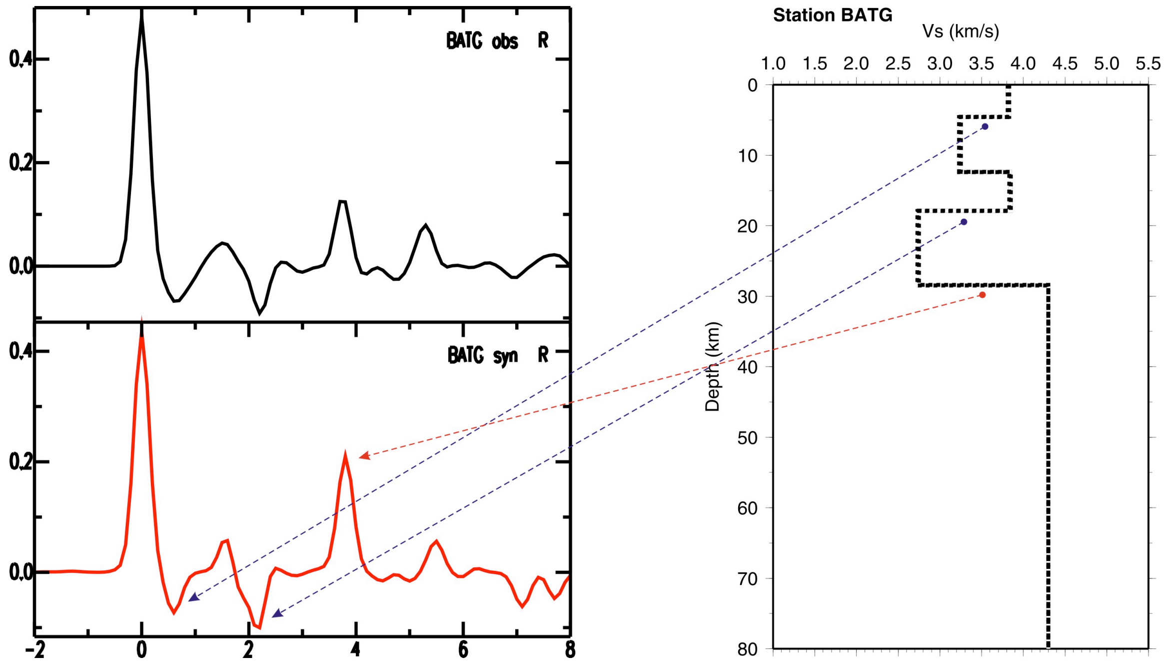

Figure 28. Receiver function inversion result for the station BATG. The black and red traces on the left panel correspond to the observed and synthetic receiver functions, respectively. The inverted shear-wave velocity profile, Vs, as a function of depth, is plotted on the right. Dashed lines link the inverted velocity discontinuities to their corresponding P-to-s converted phases on the receiver function.

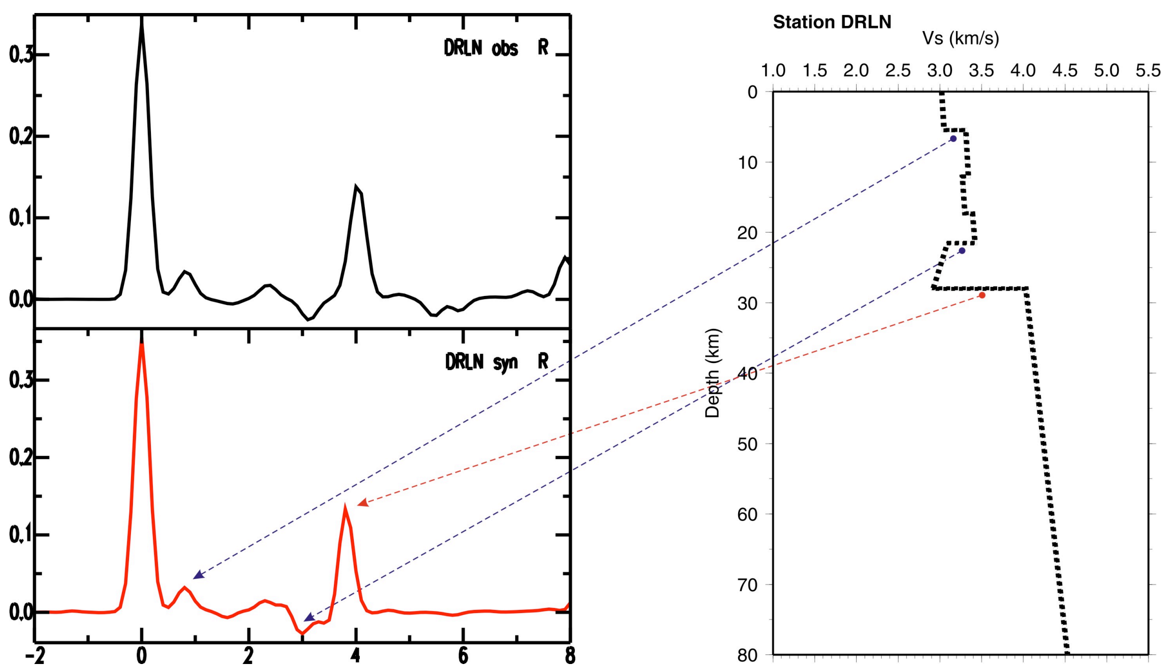

Figure 29. Receiver function inversion result for the station DRLN. Layout is the same as that in Figure 28.

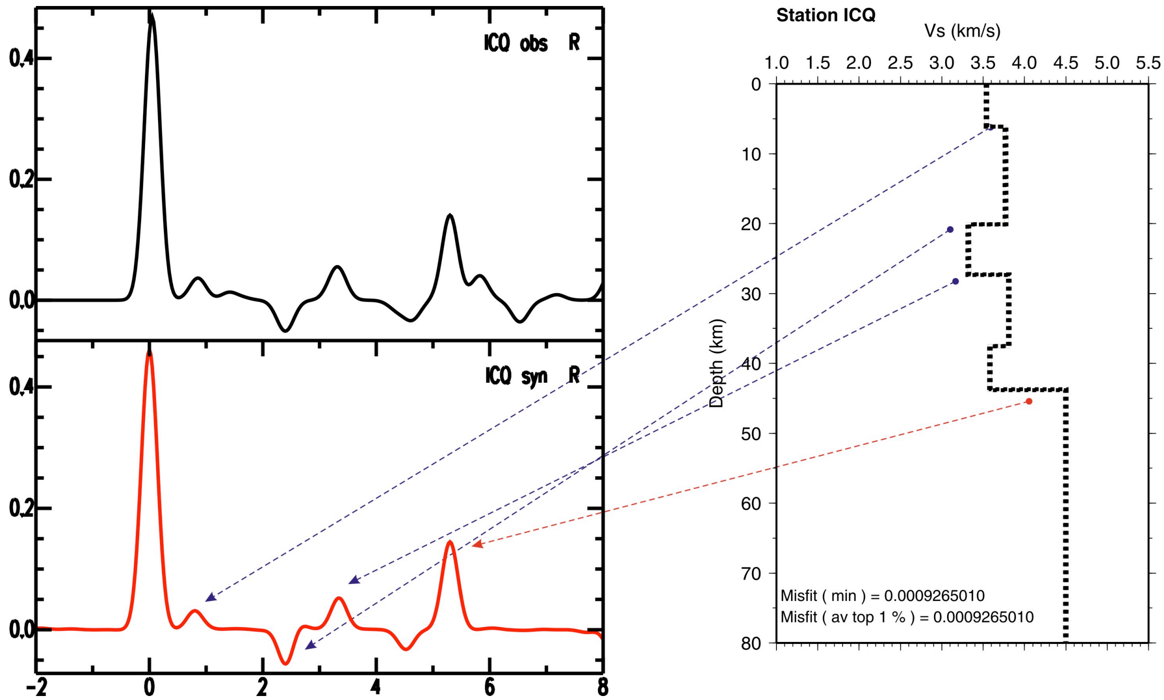

Figure 30. Receiver function inversion result for the station ICQ. Layout is the same as that in Figure 28.

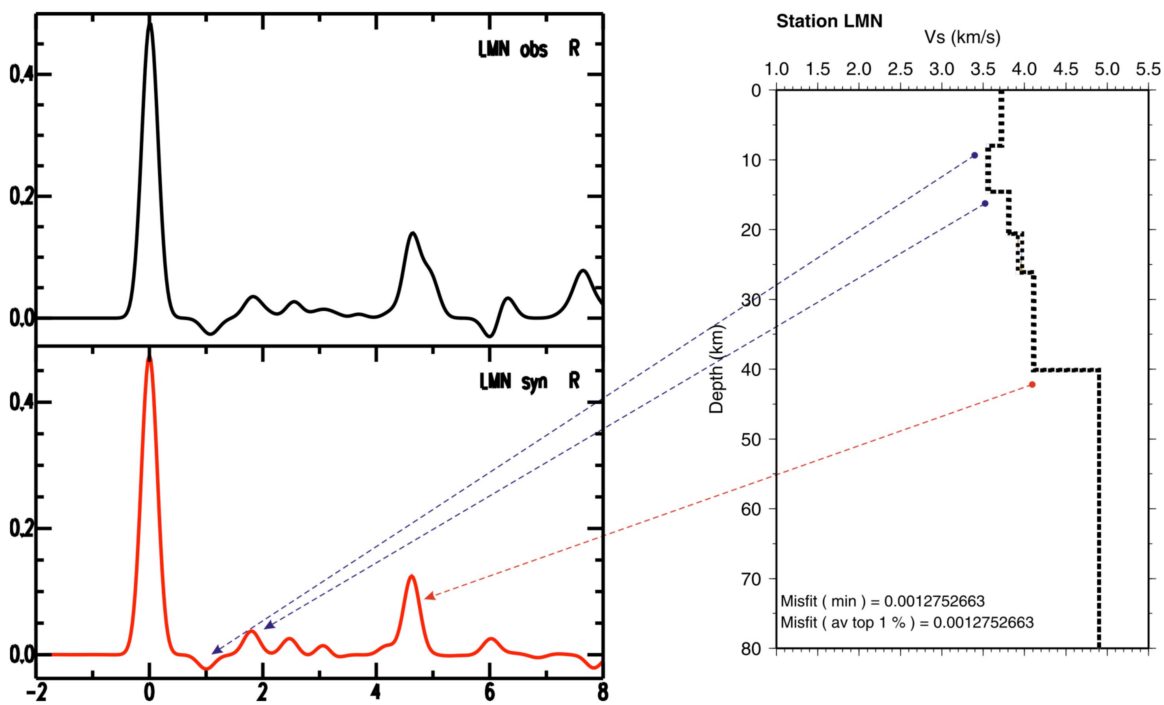

Figure 31. Receiver function inversion result for the station LMN. Layout is the same as that in Figure 28.

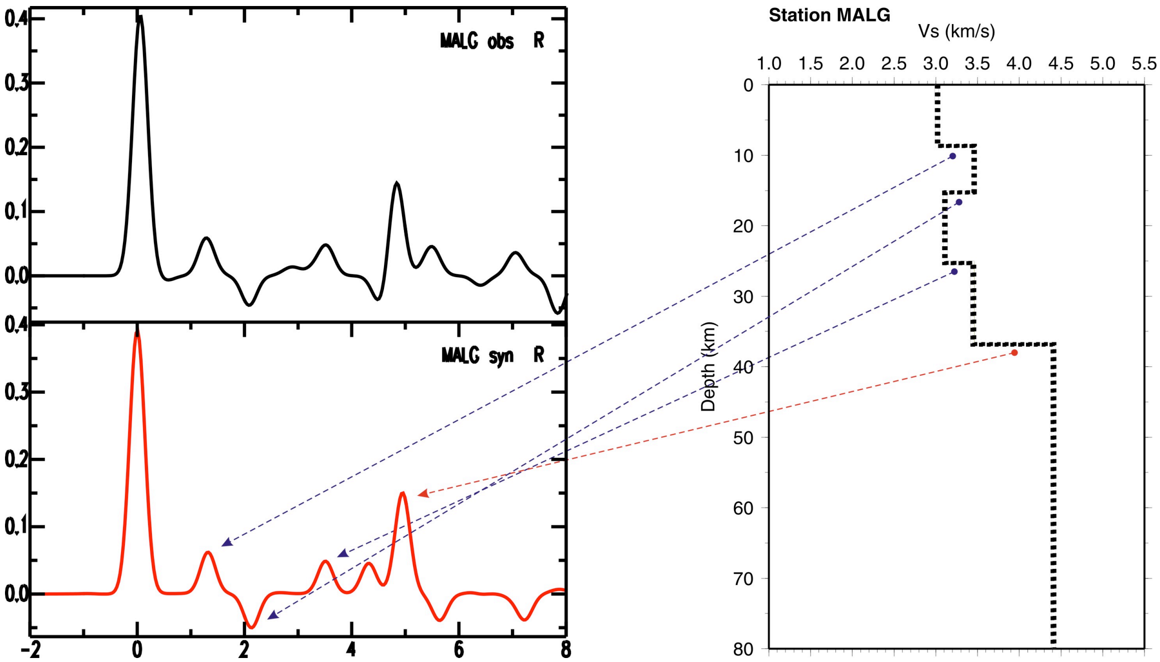

Figure 32. Receiver function inversion result for the station MALG. Layout is the same as that in Figure 28.

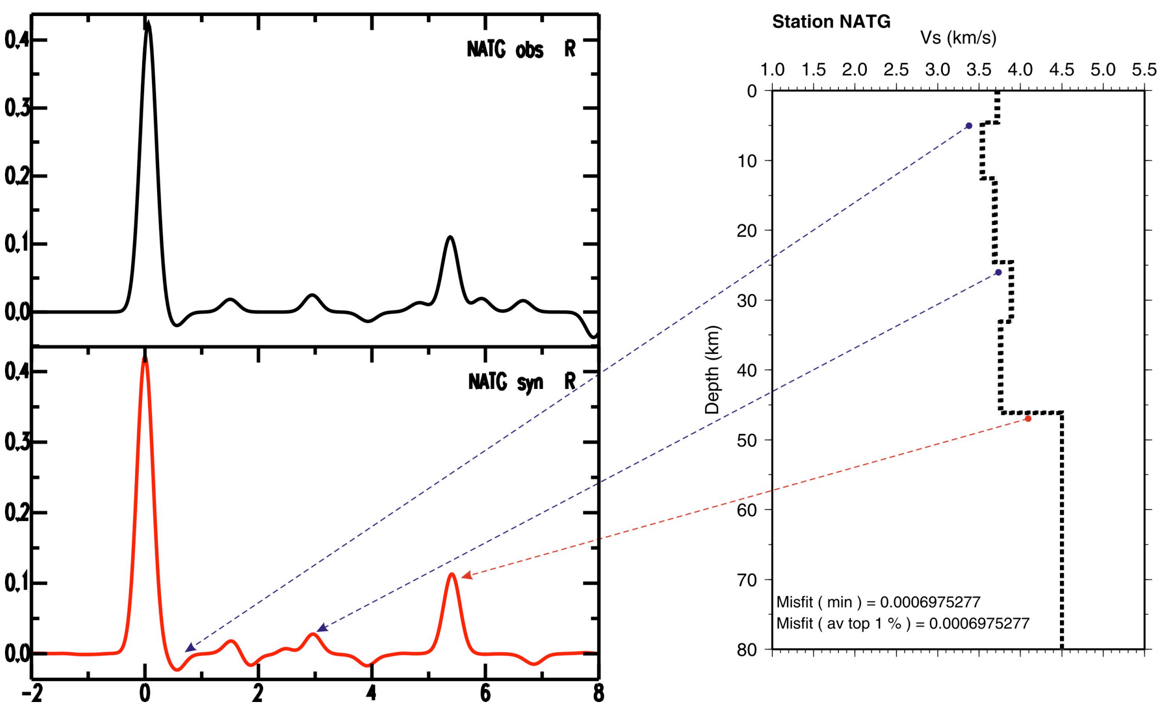

Figure 33. Receiver function inversion result for the station NATG. Layout is the same as that in Figure 28.

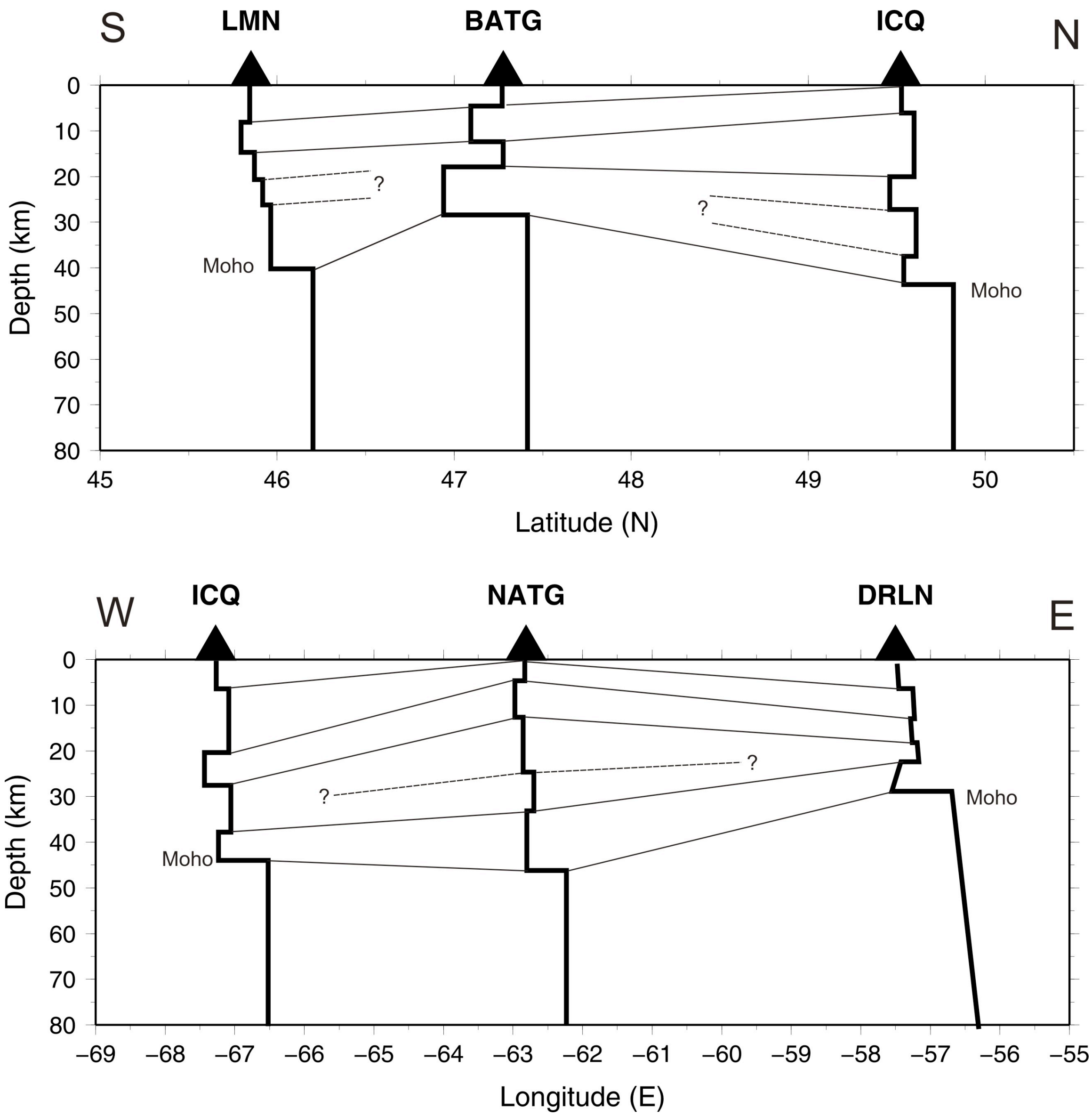

Figure 34. A schematic diagram summarizing the preliminary results of the receiver function analysis for the Gulf of St. Lawrence region. The top panel shows a north–south profile along approximately the 65°W meridian, whereas the bottom is a east–west profile along approximately the 49.5°N latitude.